No. 31 September 1977

RELATION BETWEEN SOLAR ELEVATION AND THE VERTICAL ATTENUATION COEFFICIENT OF IRRADIANCE IN OSLOFJORDEN

by

Jan H. Nilsen and Eyvind Aas

INSTITUTT FOR GEOFYSIKK

UNIVERSITETET I OSLO

INSTITUTE REPORT SERIES

No. 31 September 1977

RELATION BETWEEN SOLAR ELEVATION AND THE VERTICAL ATTENUATION COEFFICIENT OF IRRADIANCE IN OSLOFJORDEN

by

Jan H. Nilsen and Eyvind Aas

ABSTRACT

Irradiance observations at different solar elevations are presented. In the turbid waters, of coastal type 7 according to JERLOV's classification, the mean vertical attenuation coefficient in the layer 0-10 m seems to be independent of solar elevation.

CONTENTS

1: INTRODUCTION

This work is based on the thesis for the cand.real. degree by JAN H. NILSEN (1976). The variation of the vertical attenuation coefficient for downward irradiance, K, the spectral distribution of irradiance, $E_\lambda(\lambda)$, and the integrated irradiance, E, in Oslofjorden as a function of the solar elevation, h, have been investigated.

The vertical attenuation coefficient for downward irradiance at a wavelength λ, in a layer between the depths z_o and z_1, is defined as

$$K = \frac{1}{z_1 - z_o} \cdot \ln \frac{E_\lambda(\lambda, z_o)}{E_\lambda(\lambda, z_1)} \qquad 1.1$$

KOZLYANINOV and PELEVIN (1966) found for K in the upper layer of the ocean the expression

$$K = K_o \cdot D \qquad 1.2$$

where

$$K_o = \sqrt{1 - \left(\frac{b_b}{a+b_b}\right)^2} \cdot (a+b_b) \approx a+b_b \qquad 1.3$$

a = absorption coefficient; b_b = backward scattering coefficient; D = downward distribution function (TYLER and PREISENDORFER, 1962).

a and b_b are inherent optical properties and are independent of the light conditions. D, however, and consequently K, are functions of the radiance distribution.

If the radiance distribution in the sea has a strong maximum in the direction of the solar radiance, the function

D may be approximated by sec j, where j is the zenith angle of the refracted sunrays. sec j is given as a function of the solar elevation h from SNELL's law of refraction in the form

$$\sec j = \left(1 - \frac{1}{n^2} \cdot \cos^2 h\right)^{-\frac{1}{2}} \qquad 1.4$$

where n is the refractive index of sea water ($n \approx 4/3$).

It has been tested whether the secans relation

$$K(h) = K_o \cdot \sec j \qquad 1.5$$

was valid during the day of the measurement. K_o is the vertical attenuation coefficient with a zenith sun. The result has been compared with the findings of other authors. Finally the best estimate of K(h) in Oslofjorden is discussed.

2. INSTRUMENTS AND BOAT

The irradiance meter

The irradiance meter was a simple instrument consisting of a selenium cell, protected by a brass housing and a glass window. The window was covered by exterior filters of different colours with an opal glass at the top. The photocurrent from the selenium cell was recorded on deck by means of a cable and a microampere meter.

The irradiance meter was calibrated against an instrument calibrated earlier by AAS (1969, 1971).

A deck photometer with opal glass and neutral glassfilter, placed on the roof of the cabin to avoid shadows and light reflections from the boat, was used as a reference for the light conditions in air.

The Tyndall meter

Fluorescence F and scatterance $\beta(45^{\circ})$ were measured with a Tyndall meter, in values relative to a plexiglass standard (JERLOV, 1953, HØJERSLEV, 1971). The instrument consisted of a water sample section between a Hg-lamp section and a photo multiplier section. The receiver was able to measure in two different directions, 45° and 90° from the incoming rays of the lamp.

The scattered light from the water sample was measured at 45° angle. A calibration of the standard at the Institute of Physical Oceanography in Copenhagen, makes it possible to relate the $\beta(45^{\circ})$ values in relative units to the scattering coefficient b in absolute units. The scatterance data presented in Table 3 represent red light (640 nm).

The fluorescence (Table 3) was measured at an angle of 90°. The water sample was irradiated by light of wavelength 366 nm, and the light from the fluorescent matter was separated from the former light by means of a V9 filter in front of the photo multiplier.

The water sampling bottles

The water samples were collected with NIVO bottles of plastic to avoid particle contamination from the bottles.

The salinity-temperature bridge

This instrument was manufactured by Electronic Switchgear Ltd., type M.C.5.

The boat

The boat had a lenght of 9 meter. The irradiance meter was kept on a 3 meter long bar outside the boat.

3. THE STATION

The measurements were carried out between two small groups of islands, Ildjernet and Steilene, in the inner Oslofjord (Fig. 1). The place was chosen partly because of its relatively high transparency compared to the rest of the fjord at that time. The Secchi depth was 6 m on the day of the basic irradiance measurements, July 19, 1973. The depth to the bottom was 60 m. The irradiance was measured down to 30 m.

4. THE OPTICAL AND HYDROGRAPHICAL CONDITIONS

The submarine irradiance at a certain wavelength and at a certain depth is a function of cloudiness, solar elevation, turbidity of the air, state of the sea surface and inherent optical properties of the water.

It was therefore desirable to choose a day and a station where all these factors, except the solar elevation, changed as little as possible. Such ideal conditions were not easy to find, and the day of measurement was a bit cloudy (Table 1). During the summers of 1973 and 1974, however, few days had so many hours of sunshine as July 19, 1973.

The wind speed and the waves were highest when the solar elevation was 21^{o} (at 1800 hrs). Some foam also drifted on the surface, which may have caused a decrease in the submarine irradiance and perhaps also influenced the vertical attenuation coefficient, due to a more diffuse radiance distribution.

Observations of clouds together with wind speed and direction, made at Fornebu, ca. 7 km north of the station (Fig. 1) are presented in Table 1. At 1400 hrs. local time the cloudiness was 3/8 while from 1500 hrs. to 2200 hrs. it was 2/8. The dominating clouds were of Cumulus type. It was always taken great care to make the measurements when no clouds were in front of the sun. It is therefore assumed that the clouds on this day had no vital influence on the secans relation, but the clouds may slightly have caused an increase in the irradiance.

The water masses at the station were strongly stratified both hydrographically and optically as seen in Figs. 2 and 3 and Tables 2 and 3.

The isohalines and isoterms, shown in Fig. 2 as functions of time, indicate no essential change of the waters in the surface layer during the day. But the small vertical movements of the transition layer, where the optical properties changed quickly with depth, may have influenced the irradiance attenuation.

However, since we are not able to estimate the influence of the above-mentioned factors on the vertical attenuation coefficient, all variation will be attributed to the effect of solar elevation.

5. OBSERVATION AND CALCULATION OF THE SPECTRAL IRRADIANCE

Irradiance was measured with the filter combinations U1+B12, B12+G5, V9, R1 and R5, together with measurements of salinity, temperature, scatterance and fluorescence. The photocurrent from the selenium cell, p, from this date are plotted as a function of the deck photocurrent p_d, at each depth in Fig. 4-8. p and p_d are also given in Table 5. p was corrected for "dark current", which was of order 0.001 μA.

The photocurrent just below the surface was determined by measuring p with wet filters in air, and multiplying p by a coefficient including the effect of wet filters, the immersion coefficient (AAS 1969) and the surface transmittance. The values in Table 4 refer to the instrument of the Institute of Marin Research, Bergen.

At 48° solar elevation p was unfortunately not measured in air with the filter combination V9 and R1. Approximated values were found by extrapolation; the dotted lines in Figs. 6 and 7.

The instrument had to be lowered five times for each series of measurements, which then might last 40 minutes. During this time both p and p_d could change, especially for low solar elevations. In order to calculate the irradiance at a fixed solar elevation, it was therefore necessary to correct the photocurrents to the same solar elevation or to the same deck photometer reading. This was done by drawing straight lines between the points in Figs. 4-8, and then reading off the values on this line corresponding to the chosen value of p_d.

From Figs. 4-8 it is seen that there are few observations at the lowest values of p_d, that is at the lowest solar elevations which change fast. In order to get a better view of the relationship between p and p_d in this region, new sets were measured (with a different irradiance meter) on June 16 and September 12, 1974 (Figs. 9-11). The results show that the linear interpolation is a reasonable method also at low solar elevations. The interpolated photocurrents were then used to calculate the spectral irradiance distribution $E_\lambda(\lambda)$ in the different depth (AAS, 1971). The results, presented in Figs. 12-16, show that some of the spectral irradiance distributions are more irregular than others. This may be due to irregular changes in the light conditions in air, or changes in the optical properties of the water, but most probably to the uncertainty of the photocurrent readings. The distributions are also given in Table 6.

6. THE INTEGRATED IRRADIANCE

E is the irradiance integrated in the visible part of the spectrum:

$$E = \int_{350\text{ nm}}^{750\text{ nm}} E_\lambda(\lambda)d\lambda \qquad 6.1$$

E was calculated at each depth as a function of solar elevation or time, as shown in Figs. 18 and 19 and Table 7. It is notable that E decreases rapidly as the solar elevation decreases from 7° to -2°.

Fig. 17 shows the solar elevation as a function of local time in Oslo at summer and winter solstice and at the vernal and autumnal equinox (BRAHDE 1970). On the basis of this figure and Fig. 18, E is then calculated for these days in the depths 0 m, 4 m, 10 m and 20 m, assuming the optical conditions to be only a function of solar elevation. The results are presented in Figs. 20-22 and Table 8.

The total diurnal energy per unit area, $\int E\,dt$, for the mentioned five days has been calculated too, and the results are given in Table 9.

7. OPTICAL CLASSIFICATION

Table 6 shows that the maximum irradiance transmittance is 1.5% at 550 nm between 0 and 10 m depth. From 10 to 20 m the maximum transmittance is 11% at 535 nm. According to JERLOV's classification of coastal waters (e.g. 1976 tab. XXVI), these values suggest that the waters are of coastal type 6-7 and 3-4 in the upper and lower layer respectively. JERLOV's classifications refers to a solar elevation of 45° and the upper 10 meters. We have assumed that the classification values may also be used at 48° elevation and below 10 m depth.

If the irradiance transmittance of blue light (465 nm) is considered, we obtain similarly coastal waters of type 6-7 above 10 m, and type 4-5 below.

It is assumed that the visible irradiance integrated between 350 and 750 nm, at 0 meter depth represents approximately 50% of the total spectrum from 300 to 3000 nm. Also it is assumed that only wavelengths between 350 and 750 nm contribute to E at 10 and 20 m depth. From Table 7 it can be seen that at 48° solar elevation, only 0.20% of the total irradiance has reached down to 10 m, while 6.5% of the 10 m irradiance has reached down to 20 m. According to JERLOV (1976 tab.XXVIII), with the same assumptions as before, the water on the station should then be coastal water of type 7 between 0 and 10 m, and type 4 below. The results of the three different methods of classifying waters agree fairly well with each other, and we conclude that we have coastal water of type 7 above 10 m, and coastal water type 4 below.

8. CALCULATION OF THE VERTICAL ATTENUATION COEFFICIENT

If K were constant in a layer, the points obtained by plotting the irradiance in a logarithmic scale as a function of depth in a linear scale, should lie on a straight line.

In Figs. 23-26 straight lines with the best fit are drawn between the points $(z, E_{\lambda}(\lambda))$. Values of $E_{\lambda}(380\text{ nm})$, $E_{\lambda}(470\text{ nm})$, $E_{\lambda}(520\text{ nm})$ and $E_{\lambda}(620\text{ nm})$ are only used at depths where the photocurrents of U1+B12, B12+G5, V9 and R1-R5 respectively have been observed. The coefficient K seems to attain one value in the layer from 0 to 10 m, other values below. The hydrographical and optical stratification confirms this division into two layers as already seen in Fig. 3.

The relative standard deviation of K in a layer was calculated from the expression:

$$\frac{S_K}{K} = \frac{|\log E_{\lambda}(z) - \log E_{\lambda F}(z)|_{max}}{(\log E_{\lambda max} - \log E_{\lambda min}) \cdot \sqrt{\frac{N}{3}}} \qquad 8.1$$

(RASMUSSEN, 1964, p.92). The numerator in 8.1 expresses the maximum distance from the calculated irradiance E_{λ} to the point on the straight line, $E_{\lambda F}$, in the same depth. $E_{\lambda\ max}$ and $E_{\lambda\ min}$ are the greatest and smallest calculated irradiance values in the layer. N is the number of observations in the layer.

K is calculated from the straight line by eq. 1.1. The value of K, together with its standard deviation and its mean value through the day, $\overline{K}$, is plotted as a function of the solar elevation in Fig. 27. K and S_K are also presented in Table 10.

K_o is calculated from equation 1.5, and the standard deviation of K_o is calculated from the assumption

$$\frac{S_{K_o}}{K_o} = \frac{S_K}{K} \qquad 8.2$$

K_o with standard deviation and the mean value of K_o through the day, $\overline{K}_o$, are plotted in Fig. 28.

9. EARLIER INVESTIGATIONS

According to KOZLYANINOV and PELEVIN the secans relation should be valid down to an optical depth τ given by

$$\tau = cz \leq 2.5 \qquad 9.1$$

c is the (beam) attenuation coefficient.

From equation 1.3 we get

$$K_o \approx a+b_b < a+b = c \qquad 9.2$$

b is the total scattering coefficient.

Eq. 9.1 combined with 9.2 gives

$$z \leq \frac{2.5}{c} < \frac{2.5}{K_o} \qquad 9.3$$

The inequality 9.3 shows that a necessary, but not sufficient condition, is that the depth must be less than $2.5/K_o$ for the secans relation to be valid. With Table 11 the depths $2.5/\overline{K}_o$ become 1, 4, 7 and 5 m at the wavelengths 380, 470, 520 and 620 nm respectively. This means that K should not follow the secans relation entirely at any wavelength in the layer 0-10 m. The deviation, however, should be smallest at 520 nm. In the layer below 10 m depth the relation definitely should not be applicable.

JERLOV and NYGÅRD (1969) found the secans relation valid down to an optical depth

$$\tau = cz \leqq 4 \qquad 9.4$$

for blue light in the Sargasso Sea as well as for green light in the Baltic Sea. When applied to our $\overline{K}_o$ data the lower limit of validity should then be less than 7 and 11 m at the wavelength 470 and 520 nm respectively. An attempt to estimate c from the K_o values, and thus to make better use of the inequalities 9.1 and 9.4, is made in the next chapter.

It should be noted that regardless of depth HØJERSLEV found little dependence of K upon the solar elevation for green light in the Baltic Sea when the sun was lower than 40^o (1974a), and for blue light in the Mediterranean when the sun was lower than 50^o (1974b).

It may be added that AAS (1976) has proposed a formula for the vertical attenuation coefficient of blue light in the ocean. When applied to the turbid waters of Oslofjorden, this formula will give a constant K in the upper 10 meter layer.

10. ESTIMATES OF c FROM K_o

The attenuation coefficient c may be divided into

$$c = c_w + c_y + c_p \qquad 10.1$$

where c_w = attenuation coefficient due to pure water

c_y = attenuation coefficient due to yellow substance

c_p = attenuation coefficient due to particles.

The attenuation coefficient may again be divided into the absorption and scattering coefficients

$$c = a_w + a_y + a_p + b_p = a_w + a_y + a_p(1+\gamma) \qquad 10.2$$

Since $b_w << a_w$ and $b_y << a_y$, they are omitted here. γ is defined as

$$\gamma = b_p/a_p \qquad 10.3$$

According to JERLOV (1976, table IX) the backward scattering coefficient in surface ocean waters is about 2% of the total scattering coefficient. Since $b_w << b_p$ and consequently $b \approx b_p$, eq. 1.3 may be written

$$K_o \approx a+b_b = a_w+a_y+a_p+0.02\ b = a_w+a_y+a_p(1+0.02\gamma) \qquad 10.4$$

When a_y is assumed zero in the red part of the spectrum, and the definition

$$\delta_\lambda = \frac{a_{p\lambda}}{a_{p\ 655}} \qquad 10.5$$

is introduced, eqs. 10.2-5 may be solved to give a_p, b_p, a_y and c as functions of K_o:

$$a_{p\lambda} = \delta_\lambda \frac{(K_o-a_w)_{655}}{1+0.02\ \gamma_{655}} \qquad 10.6$$

$$b_{p\lambda} = \gamma_\lambda \delta_\lambda \frac{(K_o-a_w)_{655}}{1+0.02\ \gamma_{655}} \qquad 10.7$$

$$a_{y\lambda} = (K_o-a_w)_\lambda - \delta_\lambda(1+0.02\ \gamma_\lambda) \frac{(K_o-a_w)_{655}}{1+0.02\ \gamma_{655}} \qquad 10.8$$

$$c_\lambda = K_{o\lambda} + 0.98\ \delta_\lambda \gamma_\lambda \frac{(K_o-a_w)_{655}}{1+0.02\ \gamma_{655}} \qquad 10.9$$

From the results of JERLOV (1974, 1976 table XV) and HØJERSLEV (1974a) the following mean relations have been adapted

$$b_{p\ 655} \approx 2.2\ a_{p\ 655} \qquad 10.10$$

$$b_{p\ 380} \approx 1.1\ b_{p\ 655} \qquad 10.11$$

$$b_{p\ 525} \approx 1.2\ b_{p\ 655} \qquad 10.12$$

$$(a_p + b_p)_{380} \approx 1.8\ (a_p + b_p)_{655} \qquad 10.13$$

$$(a_p + b_p)_{525} \approx 1.3\ (a_p + b_p)_{655} \qquad 10.14$$

These equations can be solved for γ and δ at the different wavelengths. The results are listed in Table 12. The values for blue light (470 nm) are interpolated. $\overline{K}_o$ has been calculated from observations (Table 11), and c_w or a_w are known from tables (e.g. JERLOV 1976, table XIII). The values of γ and δ at 655 nm have been assumed valid also at 620 nm. All the terms in eq. 10.2 are then known, and the resulting values of c are presented in Table 12.

An interesting result of these very rough estimates, is that the mean value of b in the layer 0-10 m should be 0.36 m^{-1} for red light, which agrees well with the observed value at 5 m depth (Table 3), - 0.29 m^{-1}.

11. DISCUSSION

With the values of c found in the last chapter, the secans relation should not be valid below 1, 2, 3 and 3 m at 380, 470, 520 and 620 nm respectively according to KOZLYANINOV and PELEVIN, while the result of JERLOV and NYGÅRD says that it should not be valid below 4 and 5 m at 470 and 520 nm respectively, provided the results of these authors can be applied to the turbid waters of Oslofjorden. This agrees well with the results shown in Fig. 28. If a necessary condition for the secans relation to be valid is that all $K_o \pm S_{K_o}$ shall touch the line $\overline{K}_o$, then the relation definitely is not valid in the layer 0-10 m for any wavelength. (At 380 nm the standard deviation is too large and the data too scarce to test the validity, but since the relation is not valid at 470 nm, it is most probably not valid at 380 nm either).

However, from Fig. 27 it is seen that the assumption

$$K = \text{constant} = \overline{K} = \frac{1}{N}\sum^{N} K \qquad 11.1$$

would give better results than the secans relation

$$K = \overline{K}_o \sec j = \left(\frac{1}{N}\sum^{N} \frac{K}{\sec j}\right) \sec j \qquad 11.2$$

in Fig. 28. Table 13 shows the ratios $K/\overline{K}$ and $K/(\overline{K}_0 \sec j)$, and it is seen that the former ratio has the smallest deviation from 1.

We then conclude that in waters with as high vertical attenuation coefficients as those in Oslofjorden, a good assumption is that the coefficient is independent of the solar elevation.

From the discussion in Chapter 4, however, it may be argued that a weak point of this and all other similar investigations so far, is that the conclusion is based on only one day's measurements, which makes it difficult to separate the effect of solar elevation from that of other varying factors.

ACKNOWLEDGEMENTS

We are due thanks to the Institute of Marin Research, Bergen, and the Institute of Marine Biology and Limnology, University of Oslo, for instrumental support.

REFERENCES

AAS, E., 1969. On submarine irradiance measurements. Rep. Inst. Fysisk Oceanogr., Univ. Copenhagen. 6. 23 pp.

AAS, E., 1971. The natural history of the Hardangerfjord. 9. Irradiance in Hardangerfjorden 1967. Sarsia. 46: 59-78.

AAS, E., 1976. The vertical attenuation coefficient of submarine irradiance. Rep. Inst. Geofysikk, Univ. Oslo. 19. 28 pp.

BRAHDE, R., 1970. Solas stilling i Norge. Universitetsforlaget, Oslo. 215 pp.

HØJERSLEV, N.K., 1971. Tyndall and fluorescens measurements in Danish and Norwegian waters related to dynamical features. Rep. Inst. Fysisk Oceanogr. Univ.Copenhagen. 16. 46 pp.

HØJERSLEV, N.K. 1974a. Inherent and apparent optical properties of the Bàtic. Rep. Inst. Fysisk Oceanogr. Univ. Copenhagen, 23. 41 pp.

HØJERSLEV, N.K. 1974b. Daylight measurements for photosynthetic studies in the western Mediterranean. Rep.Inst.Fysisk oceanogr., Univ.Copenhagen, 26. 38 pp.

JERLOV, N.G., 1953. Particle distribution in the ocean. Rep. Swed. Deep-Sea Exped. 3: 73-97.

JERLOV, N.G., 1974. Significant relationships between optical properties of the sea. In: N.G. JERLOV and E. STEEMANN NIELSEN (editors), Optical aspects of oceanography. Academic press, New York, N.Y: 77-94.

JERLOV, N.G., 1976. Marine optics. Elsevier, Amsterdam. 231 pp.

JERLOV, N.G. and NYGÅRD, K., 1969. Influence of solar elevation on attenuation of underwater irradiance. Rep. Inst. Fysisk Oceanogr., Univ. Copenhagen. 4. 6 pp.

KOZLYANINOV, M.V. and PELEVIN, V.N., 1966. On the application of a one-dimensional approximation in the investigation of the propagation of optical radiation in the sea. U.S. Dept. Comm., Joint Publ. Res.Ser., Rept. 36: 54-63.

NILSEN, J.H., 1976. En undersøkelse av hvordan den vertikale svekningskoeffisienten for dagslyset varierer med solhøyden i det øvre laget av sjøen. Thesis, University of Oslo. Unpublished.

RASMUSSEN, R.E.H., 1964. Elementær måleteori. J. Gjellerups forlag, Copenhagen. 4.ed. 130 pp.

TYLER, J.E. and PREISENDORFER, R.W., 1962. Light. In: The Sea, Vol.1, ed. M.N. Hill. Interscience Publishers, London: 397-451.

TABLE 1. CONDITIONS AT FORNEBU AND THE STATION

Date	hr.	The Station: Secchi depth (m)	The Station: Max. wave-height (m)	Fornebu: Wind Vel. (knots)	Fornebu: Wind Dir. (degr.)	Fornebu: Clouds Cloudi-ness	Fornebu: Clouds Main cloud type	Relative humidity (%)	Air. temperature (°C)
19/7	13		0.5	3	21	3	Cumulus	44	21.5
1973	19	6.0	0.5	9	19	2	"	56	21.7
	22		0.5	3	19	2	"	65	18.5
17/6	13		0.5	9	09	2	"	27	27.5
1974	19	8.5	0.5	8	16	1	"	30	23.6
	23		0.5	4	14	1	Str.Cum.	37	21.6
12/9	13		0.5	5	22	1	Cumulus	47	18.0
1974	19	5.0	0.5	1	22	1	Str.Cum.	54	15.0
	23		0.5	0	00	1	"	80	9.8

TABLE 2A. SALINITY AND TEMPERATURE

JULY 19, 1973

Time	1300		1500		1700		1900		2300	
Depth m	S °/oo	T °C	S °/oo	T °C	S °/oo	T °/C	S °/oo	T °C	S °/oo	T °C
0	21.6	22.2	21.5	22.7	21.3	22.2	21.2	21.5	21.1	20.7
1	21.5	21.4	21.5	21.6	21.3	21.5	21.2	21.4	21.1	20.8
2	21.5	21.2	21.4	21.2	21.2	21.3	21.2	21.4	21.1	20.9
4	21.5	20.9	21.4	20.9	21.3	20.9	21.2	21.4	21.1	20.9
6	21.5	20.8	21.4	20.8	21.4	20.9	21.2	20.8	21.1	20.8
7	21.5	20.7	21.5	20.8	21.4	20.8	21.3	20.8	21.1	20.8
8	21.5	20.8	21.7	20.7	21.6	20.5	21.4	20.6	21.1	20.8
10	22.8	19.1	25.5	14.4	25.2	13.6	23.4	17.4	23.8	15.5
11	25.4	14.0	26.1	12.5	26.0	12.6	25.2	13.5	24.5	14.6
12	26.5	12.5	26.8	11.9	26.8	11.8	25.9	12.7	25.7	13.1
14	27.7	11.6	27.8	11.3	28.2	11.0	27.5	11.3	27.0	11.6
16	28.4	10.6	28.7	10.6	28.7	10.4	28.5	10.4	28.0	10.4
20	29.8	9.6	30.0	9.2	29.9	9.2	29.9	9.2	29.8	9.0
25	30.7	8.1	31.5	7.8	31.2	7.6	30.9	7.7	30.9	7.6
30	31.9	7.4	31.8	7.2	31.6	7.3	31.5	7.2	31.5	7.2
35	32.0	7.2	32.1	7.3	31.9	7.2	31.8	7.1	31.5	7.1
40					32.0	7.1	31.9	7.0	31.7	7.0

TABLE 2B. SALINITY AND TEMPERATURE

	June 16, 1974						September 12, 1974					
Time	1700		18 40		21 35		14 55		17 10		18 55	
Depth m	S $^{o}/oo$	T ^{o}C	S $^{o}/oo$	T ^{o}C	S $^{o}/oo$	T ^{o}C	S $^{o}/oo$	T ^{o}C	S $^{o}/oo$	T ^{o}C	S $^{o}/oo$	T ^{o}C
0	24.8	17.1	25.1	16.0	25.0	16.3	24.8	16.6	25.0	15.3	25.0	15.2
1	24.8	16.6	25.1	16.2	25.0	16.4	25.0	15.5	25.0	15.2	25.0	15.2
2	24.9	14.8	25.1	16.1	25.0	16.4	24.9	15.3	25.0	15.1	25.0	15.2
4	24.9	14.3	25.1	14.6	25.0	15.8	25.0	15.0	25.0	15.0	25.0	15.0
6	25.3	13.5	25.2	13.8	25.1	14.4	25.0	14.9	25.1	14.8	25.0	15.0
7			25.5	13.2	25.1	14.2	25.1	15.0	25.1	14.8	25.0	14.8
8	25.7	13.0	25.7	12.9	25.1	13.7	25.2	15.0	25.1	14.8	25.1	14.8
10	26.6	12.3	26.8	12.2	25.8	12.9	25.2	14.9	25.2	14.9	25.2	14.8
11	27.9	11.4	27.4	11.8	26.8	12.2	25.2	15.0	25.2	14.8	25.3	14.9
12	28.5	11.0	27.9	11.4	27.5	11.8	25.3	15.0	25.4	14.9	25.4	14.9
14	30.0	9.8	29.5	10.2	29.1	10.5	25.8	15.1	25.6	15.0	25.8	15.0
16	30.9	9.0	30.6	9.3	31.2	9.7	26.5	15.0	26.3	15.0	26.8	14.8
20	32.2	8.0	32.2	8.2	32.0	8.2	28.9	12.6	29.2	12.2	28.9	12.7
25	33.1	7.3	33.1	7.4	32.6	7.4	31.6	8.5	31.1	9.0	31.1	9.2
30	33.3	7.0	33.3	7.0	33.2	7.0	32.5	7.4	32.5	7.5		
40	33.9	6.6					33.1	6.4	33.4	6.4	33.5	6.4

TABLE 3. SCATTERANCE AND FLUORESCENCE

DEPTH m	$\beta(45^{o})_{red}$ rel.values	b_{red} m^{-1}	F rel.values
5	5.8	0.29	1.1
11	3.4	0.17	1.1
18	1.5	0.077	0.57
40	2.3	0.12	0.64

TABLE 4. RATIO BETWEEN CALCULATED PHOTOCURRENT BENEATH THE SURFACE, p_w, AND MEASURED PHOTOCURRENT WITH WET INSTRUMENT IN AIR, p_a.

Filter	Immersion coefficient $= \frac{\text{sensitivity in water}}{\text{sensitivity in air (dry instr.)}}$	$\frac{p_w}{p_a}$
U 1 + B 12	0.76	0.91
B 12 + G 5	0.72	0.85
V 9	0.71	0.83
R 1	0.66	0.75
R 5	0.60	0.68

TABLE 5. PHOTOCURRENTS JULY 19, 1973.

Time ca. 14; $h = 48^{\circ}$

DEPTH m	U1+B12 p µA	p_d µA	B12+G5 p µA	p_d µA	V9 p µA	p_d µA	R1 p µA	p_d µA	R5 p µA	p_d µA
0	16.8	46	70	45				52	40	54
1	0.55	45	23	45	200	48	150	51	10	54
2	0.094	45	11	45	145	48	89	50	5.2	53
4	0.0035	44	2.25	45	48	48	26.7	50	1.05	53
6			0.46	46	17	47	7.2	49	0.21	53
8			0.103	46	7	47	2.25	49	0.105	53
10			0.03	46	2.9	47	0.65	49	0.03	53
12					1.65	47	0.27	49		
14					0.91	47	0.085	49		
16					0.55	47	0.031	49		
20					0.239	47	0.0048	49		
30					0.03	47				
35					0.01	47				

Time ca. 16; $h = 36^{\circ}$

DEPTH m	U1+B12 p µA	p_d µA	B12+G5 p µA	p_d µA	V9 p µA	p_d µA	R1 p µA	p_d µA	R5 p µA	p_d µA
0	17.5	35	51	33	300	34	248	31	27	30
1	0.51	35	17.5	33	120	34	87	31	3.8	31
2	0.073	35	9.5	34	86	34	45	31	1.8	32
4	0.0015	35	1.7	34	32.6	34	11	31	0.27	31
6			0.35	34	12.2	33	3.1	31	0.049	30
8			0.066	33	4.4	30	0.9	30	0.013	29
10			0.0235	33	1.9	31	0.28	32	0.0062	29
12					1.05	29	0.102	32		
14					0.6	29	0.036	33		
16					0.36	30	0.015	35		
20					0.165	29	0.006	36		
30					0.022	29				
35					0.0085	30				

Time ca. 18; $h = 21^{\circ}$

	U1+B12 p µA	p_d µA	B12+G4 p µA	p_d µA	V9 p µA	p_d µA	R1 p µA	p_d µA	R5 p µA	p_d µA
0	4.2	15	24	18	155	20	140	23	19	24
1	0.125	15	5.4	18	58	20	50	23	3.4	24
2	0.0034	14	1.85	18	33	21	21	24	1.1	24
4			0.37	17	10.7	20	6.4	23	0.135	24
6			0.079	17	4.3	20	1.3	23	0.034	24
8			0.0145	17	1.6	20	0.41	22	0.0055	24
10			0.0042	16	0.65	19	0.11	22	0.0015	24
12					0.38	19	0.039	22		
14					0.196	20	0.0163	21		
16					0.13	20	0.0061	21		
20					0.056	19	0.0026	21		
30					0.0075	20				
35					0.0039	19				

Time ca. 20; $h = 7^{\circ}$

	U1+B12 p µA	p_d µA	B12+G4 p µA	p_d µA	V9 p µA	p_d µA	R1 p µA	p_d µA	R5 p µA	p_d µA
0	1.8	5.3	6.5	4.8	39	4.3	17	3.2	1.65	2.5
1	0.038	5.2	1.9	4.5	13	4.0	8.2	3.1	0.28	2.4
2	0.0028	5.0	1.2	4.5	8.7	3.8	3.6	3.0	0.112	2.5
4			0.28	4.4	3.1	3.8	0.98	3.0	0.02	2.6
6			0.045	4.6	1.1	3.8	0.25	2.9	0.0034	2.5
8			0.01	4.5	0.36	3.7	0.064	2.9	0.0005	2.4
10			0.0035	4.4	0.138	3.7	0.017	2.9		
12					0.06	3.6	0.0046	2.9		
14					0.033	3.6	0.0018	2.8		
16					0.0178	3.5				
20					0.0074	3.6				
30					0.0015	3.5				

Time ca. 22; $h = -2^{\circ}$

0	0.0015	0.003	0.028	0.009	0.15	0.015	0.17	0.027	0.066	0.046
1			0.012	0.008	0.056	0.013	0.054	0.025	0.0085	0.043
2			0.0024	0.007	0.036	0.013	0.03	0.023	0.0031	0.038
4			0.0006	0.005	0.0125	0.013	0.005	0.022		
6					0.005	0.011	0.0005	0.021		

TABLE 6A

$E_{\lambda}(\lambda)$ in mW m^{-2} nm^{-1}. Time 1400, h = 48°.											
nm	0m	1m	2m	4m	6m	8m	10m	12m	16m	20m	30m
350	447.	5.70	.322								
360	492.	9.87	.957								
370	544.	16.9	2.61	.0420							
380	631.	29.2	5.47	.210							
390	683.	49.9	9.53	.707							
400	715.	79.6	15.2	1.51							
410	742.	114.	25.8	3.28	.133						
420	774.	156.	39.9	6.15	.301	.0291					
430	789.	205.	58.9	9.42	.743	.0722	.0131				
440	808.	249.	86.5	13.5	1.37	.161	.0341				
450	827.	309.	120.	19.1	2.87	.338	.0787				
460	832.	361.	154.	27.2	4.82	.768	.187	.0600			
470	836.	406.	194.	40.5	7.94	1.58	.412	.153	.0200		
480	840.	450.	233.	56.5	11.9	3.04	.945	.359	.0473	.0179	.00244
490	853.	476.	283.	79.5	19.9	6.13	1.92	.798	.129	.0494	.00791
500	871.	515.	346.	107.	29.5	10.1	3.45	1.70	.336	.114	.0259
510	880.	559.	403.	132.	42.1	16.5	6.07	3.07	.867	.314	.0719
520	894.	586.	437.	149.	54.5	22.6	8.44	4.83	1.77	.764	.136
530	869.	597.	451.	154.	59.7	25.8	11.1	6.59	2.56	1.23	.169
540	872.	588.	460.	157.	62.7	28.0	12.6	7.69	2.99	1.43	.154
550	855.	572.	456.	154.	63.5	28.9	12.6	7.76	2.82	1.28	.111
560	846.	533.	432.	146.	59.7	26.8	11.4	6.74	2.09	.764	.0626
570	823.	512.	390.	137.	55.2	22.8	9.92	4.97	1.26	.370	.0331
560	798.	490.	351.	126.	47.9	17.7	7.47	3.59	.793	.179	.0158
590	773.	452.	320.	112.	39.2	14.2	5.36	2.49	.447	.0858	.00791
600	746.	429.	276.	100.	31.3	10.7	3.64	1.81	.236	.0414	.00331
610	701.	387.	243.	81.8	24.7	7.48	2.49	1.13	.140	.0236	.00151
620	637.	354.	212.	65.0	18.9	5.75	1.66	.682	.0813	.0120	
630	572.	313.	184.	54.5	14.9	4.22	1.11	.432	.0450	.00651	
640	514.	269.	158.	43.2	11.4	2.87	.686	.276	.0221	.00355	
650	455.	241.	138.	35.0	8.79	1.91	.431	.155	.0118	.00177	
660	407.	196.	118.	28.1	6.25	1.43	.274	.0950	.00672	.000987	
670	378.	168.	99.6	22.2	4.43	.901	.186				
680	337.	144.	83.9	17.2	3.26						
690	301.	125.	67.8	13.8	2.21						
700	266.	106.	56.1	10.5	1.49						
710	239.	91.7	46.1	8.34							
720	210.	78.3	37.5	5.95							
730	182.		30.2								

TABLE 6B

$E_\lambda(\lambda)$ in mW m^{-2} nm^{-1}. Time 1600, h = 36°.

nm	0m	1m	2m	4m	6m	8m	10m	12m	16m	20m	30m
350	533.	4.89	.217								
360	563.	8.48	.651								
370	589.	14.5	1.75	.0124							
380	606.	25.0	3.73	.0634							
390	627.	42.8	6.51	.211							
400	640.	68.4	10.4	.451							
410	637.	95.2	18.5	1.10	.0971						
420	633.	126.	30.1	2.43	.219	.0177					
430	618.	161.	46.6	4.67	.541	.0439	.00937				
440	602.	204.	71.4	7.98	1.00	.0982	.0243				
450	582.	247.	103.	13.1	2.09	.205	.0562				
460	579.	274.	132.	19.5	3.51	.467	.134	.0453			
470	577.	300.	171.	29.1	5.78	.963	.294	.116	.0146		
480	578.	314.	194.	40.6	8.68	1.85	.675	.271	.0346	.0138	.00195
490	579.	319.	212.	56.5	14.5	3.88	1.36	.602	.0944	.0380	.00633
500	580.	324.	231.	75.7	21.6	6.71	2.45	1.28	.246	.0882	.0207
510	580.	330.	245.	92.1	30.9	11.3	4.31	2.32	.634	.242	.0575
520	581.	332.	248.	103.	40.1	16.1	5.98	3.65	1.30	.588	.109
530	581.	335.	250.	106.	44.0	18.4	7.87	4.97	1.87	.951	.135
540	578.	334.	252.	108.	46.2	20.0	8.96	5.80	2.19	1.10	.123
550	568.	326.	250.	105.	46.7	20.7	8.96	5.86	2.06	.985	.0892
560	562.	313.	236.	100.	44.0	19.1	8.15	5.08	1.53	.588	.0500
570	555.	305.	220.	88.3	37.8	15.1	6.44	3.33	.842	.294	.0264
580	544.	305.	205.	75.7	30.3	11.0	4.48	2.13	.478	.147	.0126
590	532.	295.	194.	63.1	22.7	8.38	2.99	1.30	.242	.0726	.00633
600	514.	284.	173.	52.9	16.5	5.98	1.91	.832	.113	.0363	.00264
610	488.	264.	152.	43.3	13.1	4.16	1.30	.519	.0674	.0207	.00120
620	443.	244.	133.	34.4	10.0	3.20	.884	.313	.0390	.0105	
630	408.	223.	115.	28.8	7.94	2.35	.586	.198	.0216	.00570	
640	363.	199.	99.6	22.8	6.04	1.60	.360	.126	.0106	.00311	
650	319.	169.	87.1	18.5	4.66	1.06	.226	.0713	.00568	.00155	
660	284.	149.	74.1	14.9	3.31	.801	.144	.0436	.00323	.000864	
670	257.	132.	62.4	11.8	2.34	.502	.0977				
680	233.	115.	52.6	9.15	1.72						
690	213.	93.6	42.5	7.36	1.17						
700	188.	86.4	35.2	5.57	.794						
710	168.	73.2	28.9	4.41							
720	149.	63.0	23.5	3.15							
730	128.	53.9	19.0								

TABLE 6C

$E_\lambda(\lambda)$ in mW m^{-2} nm^{-1}. Time 1800, h = 21°.

nm	0m	1m	2m	4m	6m	8m	10m	12m	16m	20m	30m
350	220.	2.07	.0380								
360	232.	3.59	.114								
370	233.	6.17	.304								
380	250.	10.6	.655								
390	259.	17.8	1.14								
400	264.	26.5	1.94	.136							
410	276.	35.9	3.62	.337	.0364						
420	288.	47.2	6.39	.744	.0822	.00537					
430	295.	58.9	10.5	1.43	.205	.0133	.00281				
440	301.	71.8	17.0	2.47	.374	.0297	.00731				
450	306.	85.6	24.4	4.09	.785	.0622	.0168				
460	304.	97.8	31.9	6.09	1.30	.141	.0402	.0163			
470	304.	111.	42.8	9.07	2.16	.291	.0883	.0417	.00468		
480	304.	122.	49.8	12.6	3.24	.560	.202	.0975	.0110	.00471	.000611
490	305.	135.	61.4	17.7	5.34	1.19	.431	.216	.0301	.0129	.00197
500	305.	145.	75.4	23.9	7.76	2.09	.812	.463	.0786	.0300	.00647
510	306.	157.	89.0	29.3	10.8	3.59	1.49	.835	.202	.0824	.0173
520	306.	170.	100.	33.0	13.8	5.18	2.16	1.31	.415	.200	.0341
530	306.	171.	100.	34.2	15.1	5.91	2.85	1.79	.599	.323	.0422
540	305.	171.	101.	34.9	15.8	6.42	3.24	2.08	.699	.376	.0386
550	300.	167.	100.	34.2	16.0	6.63	3.24	2.10	.659	.335	.0278
560	291.	158.	94.7	32.3	15.1	6.13	2.95	1.83	.488	.200	.0156
570	275.	151.	84.1	31.0	12.5	4.90	2.26	1.16	.281	.100	.00527
580	269.	146.	76.6	28.7	9.89	3.61	1.53	.718	.168	.0500	.00335
590	246.	141.	69.2	25.7	7.34	2.77	.994	.420	.0907	.0247	.00197
600	230.	134.	61.4	23.0	5.61	1.99	.616	.254	.0456	.0123	.000827
610	211.	120.	52.5	18.8	4.16	1.38	.421	.158	.0270	.00706	.000377
620	192.	109.	46.2	14.9	3.12	1.06	.285	.0956	.01567	.00359	
630	171.	96.0	39.5	12.5	2.44	.783	.189	.0605	.00869	.00194	
640	154.	86.5	34.0	9.94	1.76	.534	.116	.0387	.00427	.00106	
650	138.	76.3	28.3	8.06	1.31	.356	.0729	.0217	.00228	.000530	
660	123.	67.5	24.8	6.48	.977	.267	.0464	.0133	.00129	.000294	
670	111.	59.3	19.9	5.12	.717	.167	.0315				
680	99.9	52.0	16.8	3.97	.530						
690	89.3	44.7	13.8	3.20	.364						
700	79.3	38.8	12.0	2.42	.244						
710	71.9	32.9	9.89	1.92							
720	62.3	28.2	8.05	1.37							
730	56.0	24.1	6.48								

TABLE 6D

$E_\lambda(\lambda)$ in mW m^{-2} nm^{-1}. Time 2000, h = 7^o.

nm	0m	1m	2m	4m	6m	8m	10m	12m	16m	20m	30m
350	43.6	.282	.00819								
360	46.1	.490	.0245								
370	47.9	.843	.0652								
380	49.6	1.44	.139								
390	51.3	2.43	.256								
400	52.4	3.61	.493	.0705							
410	52.6	5.77	.996	.173	.0119						
420	52.8	8.73	2.04	.382	.0270	.00271					
430	51.7	12.3	3.59	.738	.0676	.00672	.00166				
440	50.6	16.8	6.01	1.26	.122	.0150	.00437				
450	49.1	22.3	9.48	2.09	.258	.0314	.0100				
460	48.7	25.5	14.4	3.13	.430	.0714	.0239	.00250			
470	49.9	28.9	19.7	4.66	.710	.147	.0521	.00642	.000744		
480	53.1	31.8	23.4	6.24	1.06	.283	.104	.0149	.00167	.000620	.000138
490	58.6	33.8	25.2	7.59	1.64	.508	.164	.0333	.00456	.00170	.000448
500	65.3	34.5	25.8	8.71	2.22	.738	.248	.0712	.0120	.00395	.00145
510	71.4	35.6	26.1	9.44	2.90	1.02	.339	.128	.0307	.0108	.00407
520	75.7	36.6	26.2	9.80	3.41	1.16	.426	.201	.0633	.0263	.00774
530	77.3	36.9	26.7	10.0	3.74	1.32	.518	.275	.0912	.0426	.00958
540	78.0	36.8	26.5	10.1	3.93	1.44	.590	.321	.102	.0496	.00876
550	78.0	35.9	25.8	10.0	3.97	1.48	.590	.324	.100	.0442	.00632
560	76.3	34.1	24.4	9.22	3.74	1.37	.536	.281	.0838	.0263	.00354
570	65.8	33.5	22.3	8.23	3.21	1.11	.438	.184	.0643	.0131	.00187
580	56.3	33.2	19.9	7.20	2.62	.824	.310	.118	.0455	.00659	.000897
590	48.7	32.6	17.6	6.09	2.01	.638	.216	.0723	.0306	.00325	.000448
600	41.4	31.7	16.0	5.19	1.59	.463	.142	.0462	.0210	.00162	.000187
610	37.9	28.6	13.9	4.24	1.17	.323	.0973	.0288	.0126	.000931	.0000856
620	34.5	25.9	11.9	3.37	.884	.248	.0655	.0173	.00725	.000473	
630	30.7	22.7	10.0	2.82	.692	.182	.0433	.0110	.00399		
640	27.7	20.5	8.59	2.24	.501	.124	.0264	.00704	.00199		
650	24.9	18.1	7.19	1.81	.371	.0828	.0169	.00396	.00105		
660	22.1	16.0	6.08	1.46	.277	.0621	.0105	.00242			
670	20.0	14.0	5.09	1.15	.203	.0389	.00730				
680	17.9	12.3	4.24	.893	.150						
690	16.0	10.6	3.59	.725	.103						
700	14.2	9.21	2.99	.546	.0692						
710	12.9	7.81	2.49	.431							
720	11.2	6.71	2.04	.304							
730	10.0	5.73	1.67								

TABLE 6E

$E_{\lambda}(\lambda)$ in mW m^{-2} nm^{-1}. Time 2200, h = -2^{o}.

nm	0m	1m	2m	4m	6m
350	.165				
360	.219	.00732			
370	.281	.0159			
380	.351	.0319	.00134		
390	.425	.0648	.00268		
400	.510	.122	.00492		
410	.570	.219	.00823	.00105	
420	.611	.311	.0138	.00225	
430	.651	.380	.0232	.00431	
440	.658	.409	.0384	.00735	.000589
450	.647	.418	.0590	.0133	.00147
460	.629	.409	.0850	.0211	.00314
470	.593	.389	.118	.0321	.00628
480	.548	.347	.153	.0470	.0103
490	.510	.305	.172	.0561	.0186
500	.481	.265	.178	.0611	.0260
510	.441	.234	.180	.0632	.0314
520	.400	.204	.174	.0623	.0334
530	.371	.186	.161	.0605	.0331
540	.343	.170	.148	.0558	.0299
550	.314	.158	.136	.0493	.0250
560	.285	.146	.123	.0428	.0186
570	.263	.143	.114	.0385	.0137
580	.249	.141	.105	.0328	.00982
590	.229	.136	.0962	.0277	.00687
600	.214	.130	.0861	.0222	.00451
610	.191	.119	.0747	.0169	.00314
620	.175	.109	.0653	.0126	.00196
630	.156	.0993	.0570	.00973	.00117
640	.141	.0894	.0477	.00708	.000785
650	.126	.0805	.0389	.00476	.000392
660	.112	.0717	.0311	.00359	
670	.101	.0629	.0254	.00253	
680	.0887	.0540	.0202	.00169	
690	.0763	.0463	.0160	.00116	
700	.0678	.0397	.0129	.000740	
710	.0595	.0342	.00954	.000423	
720	.0511	.0292	.00788		
730	.0449	.0248	.00622		

TABLE 7. IRRADIANCE IN THE REGION 350 - 750 nm

Depth m	E in W/m² solar elevation 48°	36°	21°	7°	-2°
0	252	188	88.5	17.7	0.124
1	112	75.7	33.9	7.76	0.062
2	70.4	44.4	15.2	4.44	0.026
4	21.2	13.6	4.74	1.49	0.008
6	6.93	4.69	1.59	0.422	0.003
8	2.62	1.75	0.561	0.137	
10	1.03	0.687	0.241	0.050	
12	0.555	0.389	0.138	0.022	
16	0.167	0.118	0.038	0.007	
20	0.067	0.052	0.018	0.002	
30	0.008	0.006	0.002	0.0005	

TABLE 8. IRRADIANCE IN THE REGION 350 - 750 nm

Date	Depth m	E in W/m² Time 12	14	16	18	20	22
June 21	0	265	250	190	96	23	0.25
	4	25	22	14	5.5	1.6	
	10	1.2	1.1	.68	.28	.060	
	20	.080	.075	.054	.021	.0030	
March 20 Sept. 23	0	135	115	54	2.5		
	4	8.5	6.8	3.2	.32		
	10	.46	.36	.13			
	20	.034	.028	.0085			
Dec. 22	0	15	7.0				
	4	1.2	.70				

TABLE 9. TOTAL DIURNAL ENERGY

Depth m	Energy in J/m² June 29	July 19	March & Sept. 23	Dec. 22
0	$9.5 \cdot 10^6$	$8.8 \cdot 10^6$	$3.4 \cdot 10^6$	$1.8 \cdot 10^5$
4	$7.5 \cdot 10^5$	$6.7 \cdot 10^5$	$2.1 \cdot 10^5$	$1.6 \cdot 10^4$
10	$3.6 \cdot 10^4$	$3.3 \cdot 10^4$	$1.0 \cdot 10^4$	
20	$2.6 \cdot 10^3$	$2.3 \cdot 10^3$	$7.7 \cdot 10^2$	

TABLE 10. K (m^{-1}) IN THE LAYER 0-10 m.

λ nm	Time	14 K	14 S_K	16 K	16 S_K	18 K	18 S_K	20 K	20 S_K	22 K	22 S_K
380		2.15	.16	2.30	.14						
470		.77	.01	.79	.01	.83	.02	.74	.01	.84	.07
520		.47	.01	.46	.01	.50	.02	.51	.01	.41	.02
620		.60	.01	.62	.01	.66	.01	.65	.03	.65	.04

TABLE 11. K_o (m^{-1}) IN THE LAYER 0-10 m

λ nm	Time	14 K_o	14 S_{K_o}	16 K_o	16 S_{K_o}	18 K_o	18 S_{K_o}	20 K_o	20 S_{K_o}	22 K_o	22 K_{S_o}
380		1.86	.14	1.83	.11						
470		.67	.01	.63	.01	.59	.01	.49	.01	.56	.04
520		.41	.01	.37	.01	.36	.01	.34	.01	.27	.02
620		.52	.01	.49	.01	.47	.01	.43	.02	.42	.03

TABLE 12. ESTIMATES OF c FROM K_o

λ nm	$\bar{K}_o$ m^{-1}	a_w m^{-1}	γ	δ	a_p m^{-1}	b_p m^{-1}	a_y m^{-1}	c m^{-1}
380	1.85	0.04	0.7	3.3	0.56	0.39	1.25	2.24
470	0.59	0.02	1.3	2.2	0.37	0.48	0.19	1.06
520	0.35	0.04	1.7	1.5	0.25	0.43	0.05	0.77
620	0.47	0.29	2.2	1	0.17	0.37	0	0.83

TABLE 13. THE RATIOS $R_1 = \frac{K}{\bar{K}}$ AND $R_2 = \frac{K}{\bar{K}_o \sec j}$ AND THEIR DEVIATION FROM 1 IN %.

λ	380 nm				470 nm				520 nm				620 nm			
TIME	R_1	%	R_2	%	R_1	%	R_2	%	R_1	%	R_2	%	R_1	%	R_2	%
14	.96	4	1.01	1	.97	3	1.14	14	1.00	0	1.17	17	.94	6	1.11	11
16	1.03	3	.99	1	1.00	0	1.07	7	.98	2	1.06	6	.97	3	1.04	4
18					1.05	5	1.00	0	1.06	6	1.03	3	1.03	3	1.00	0
20					.94	6	.83	17	1.09	9	.97	3	1.02	2	.91	9
22					1.06	6	.95	5	.87	13	.77	23	1.02	2	.89	11
MEAN % DEVI-ATION		4		1		4		9		6		10		3		7

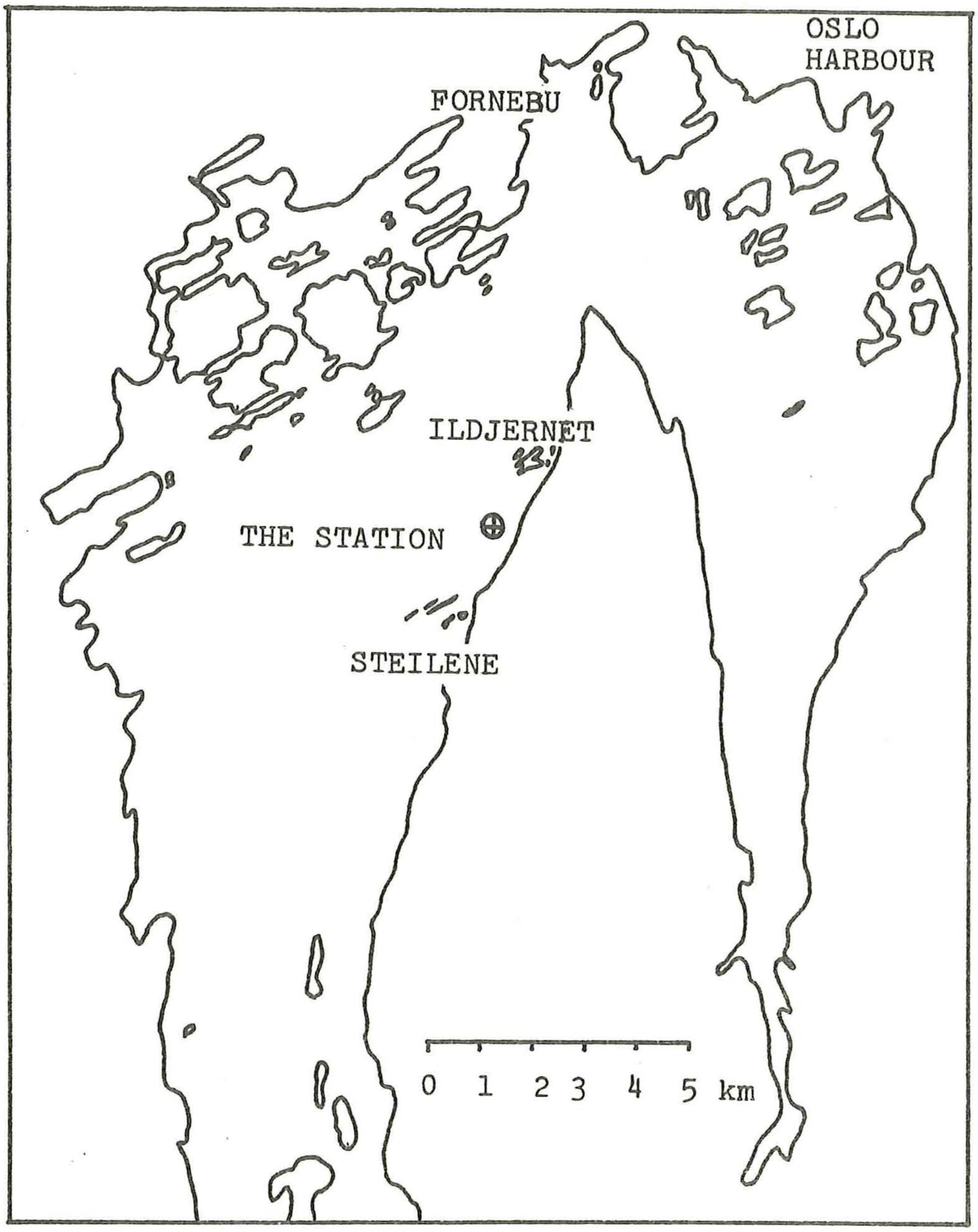

Fig.1. The location of the station in Oslofjorden.

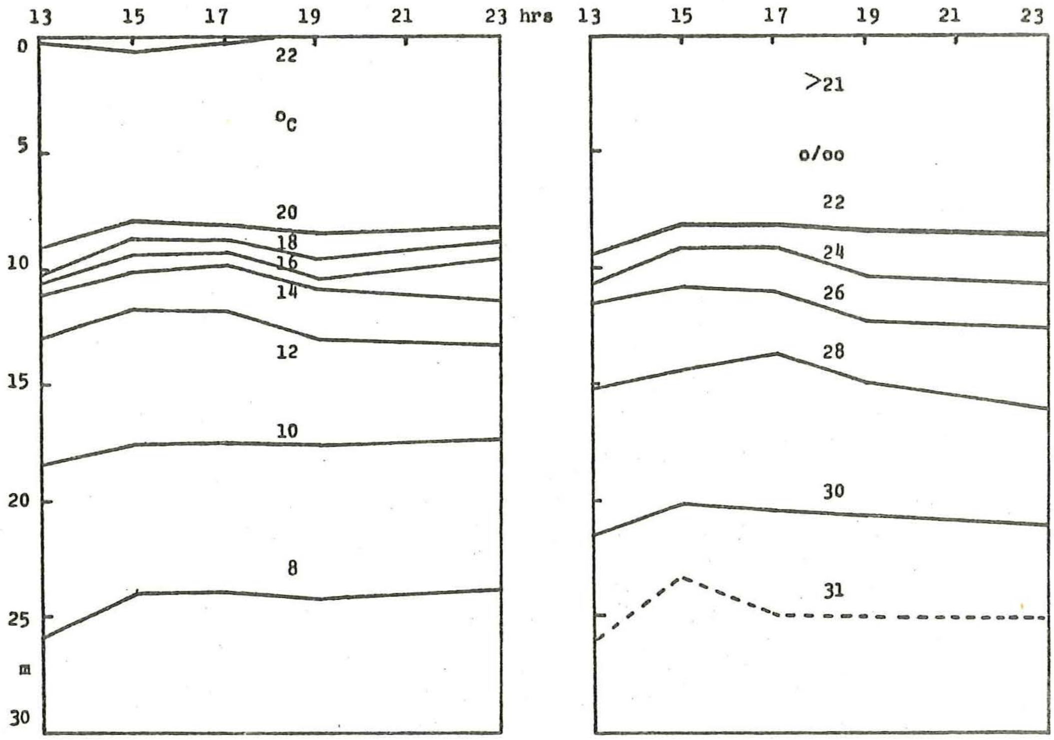

Fig. 2.
The distribution of temperature and salinity during July 19, 1973

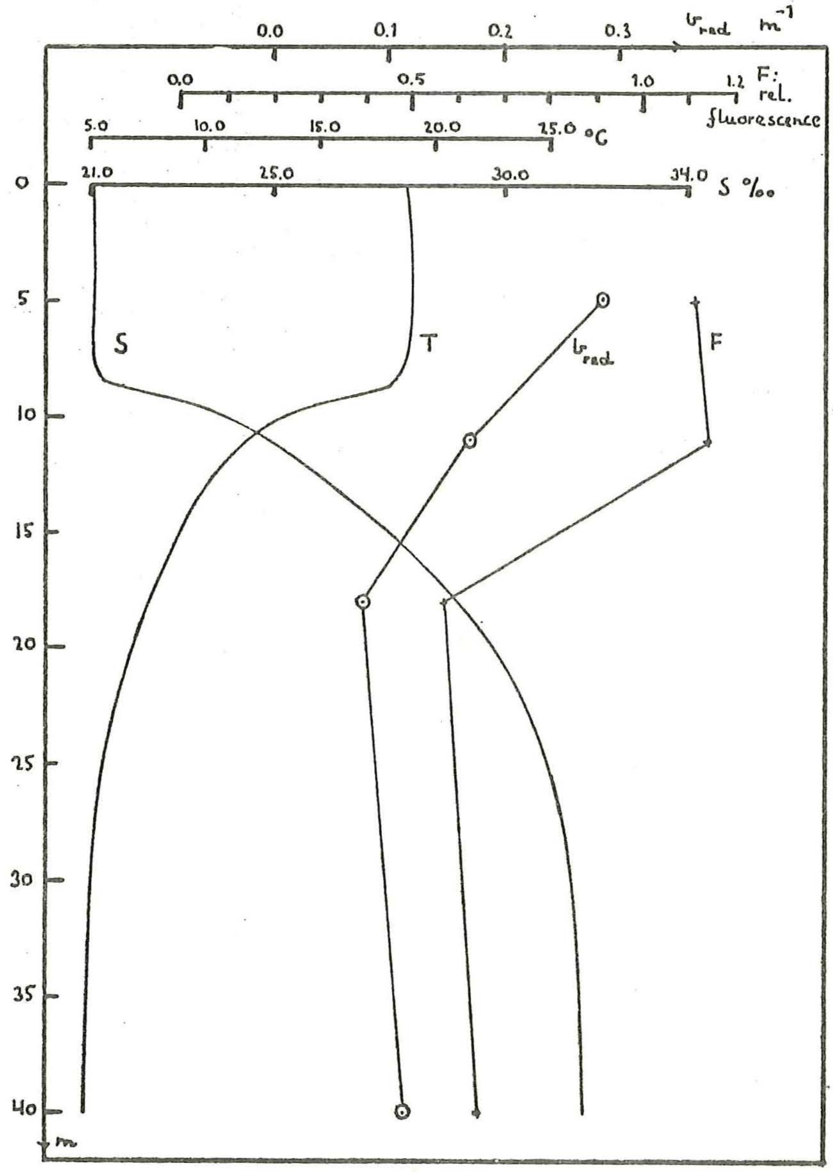

Fig. 3.
Vertical distribution of temperature, T, salinity, S, scattering coefficient, b, and fluorescence, F, at 23 hrs, July 19, 1973.

Fig. 4.
p_{U1+B12} as a function of p_d July 19, 1973.

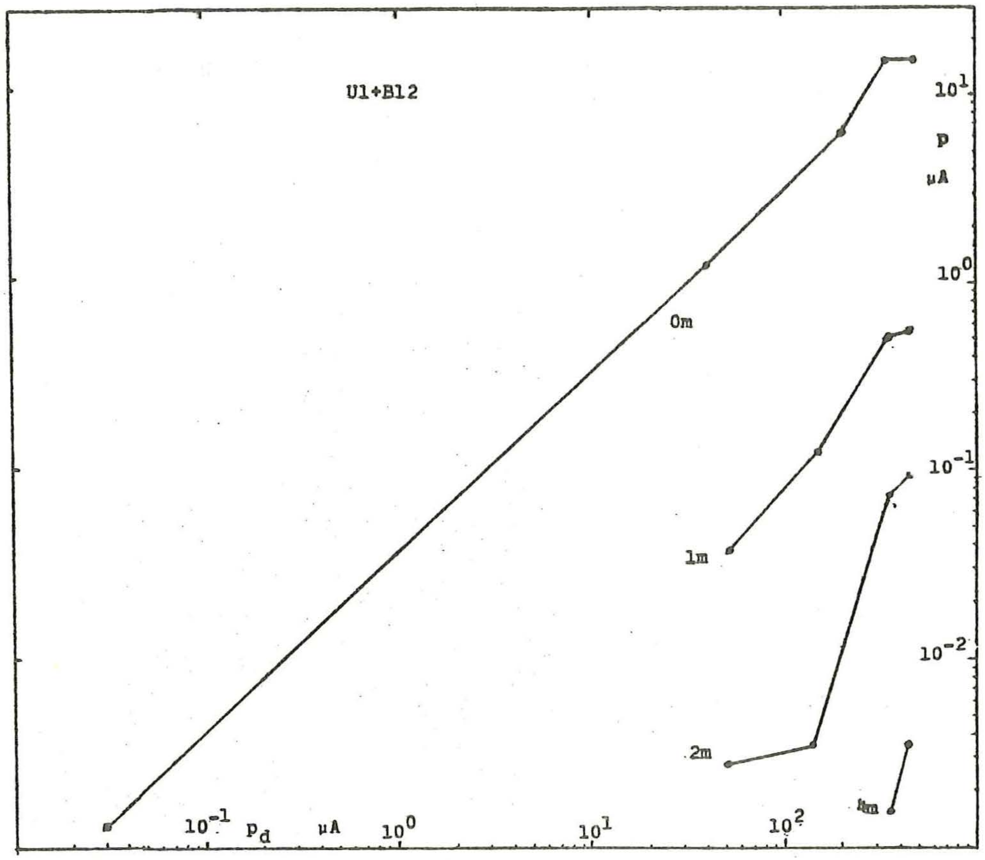

Fig. 5.
p_{B12+G5} as a function of p_d. July 19, 1973.

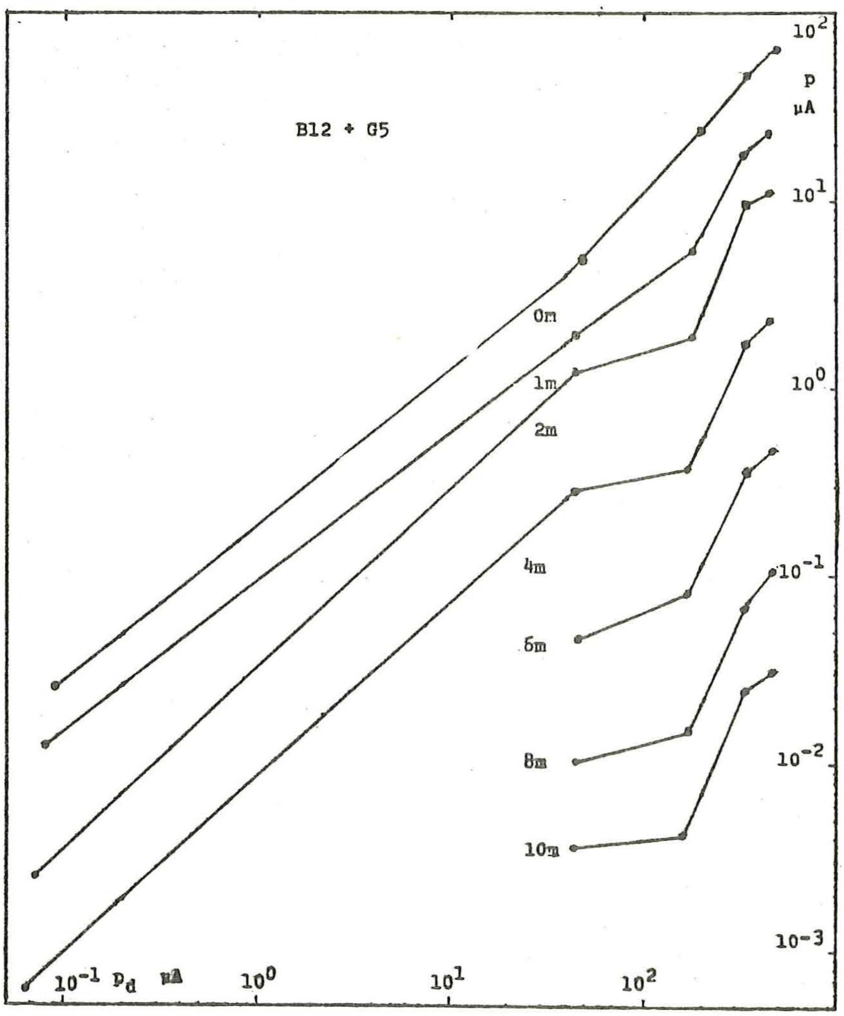

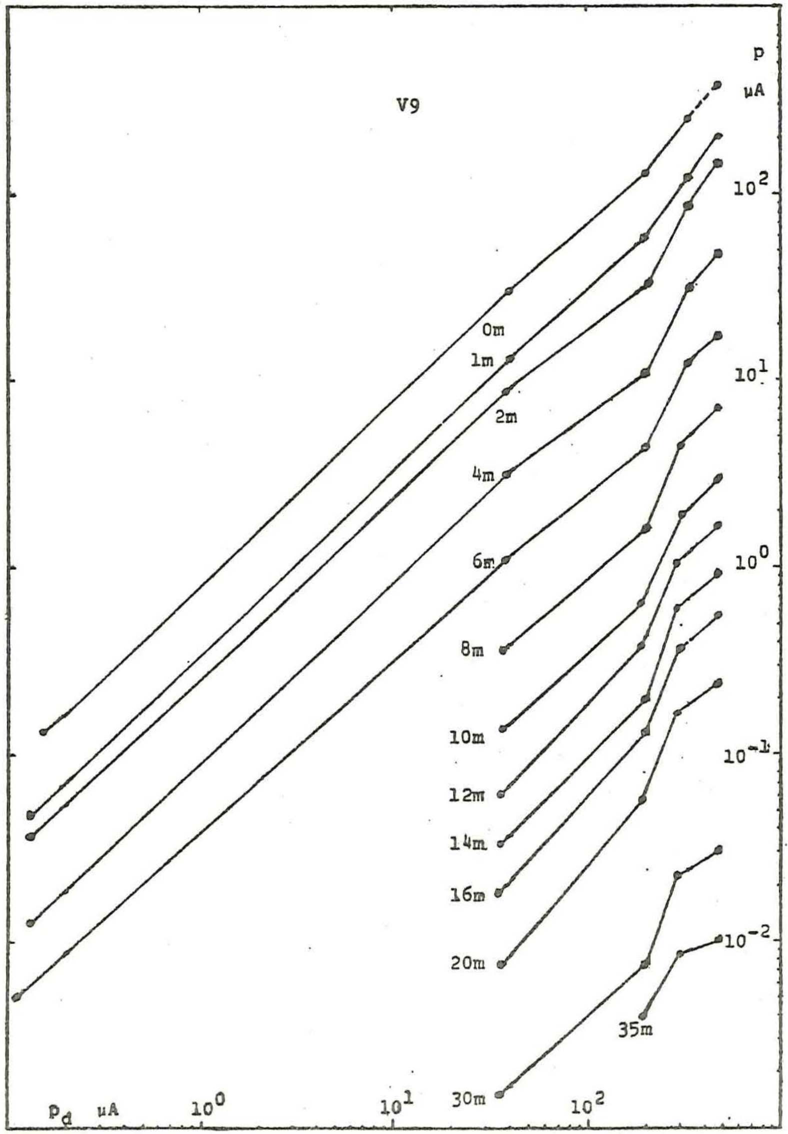

Fig. 6. p_{V9} as a function of p_d.
July 19, 1973.

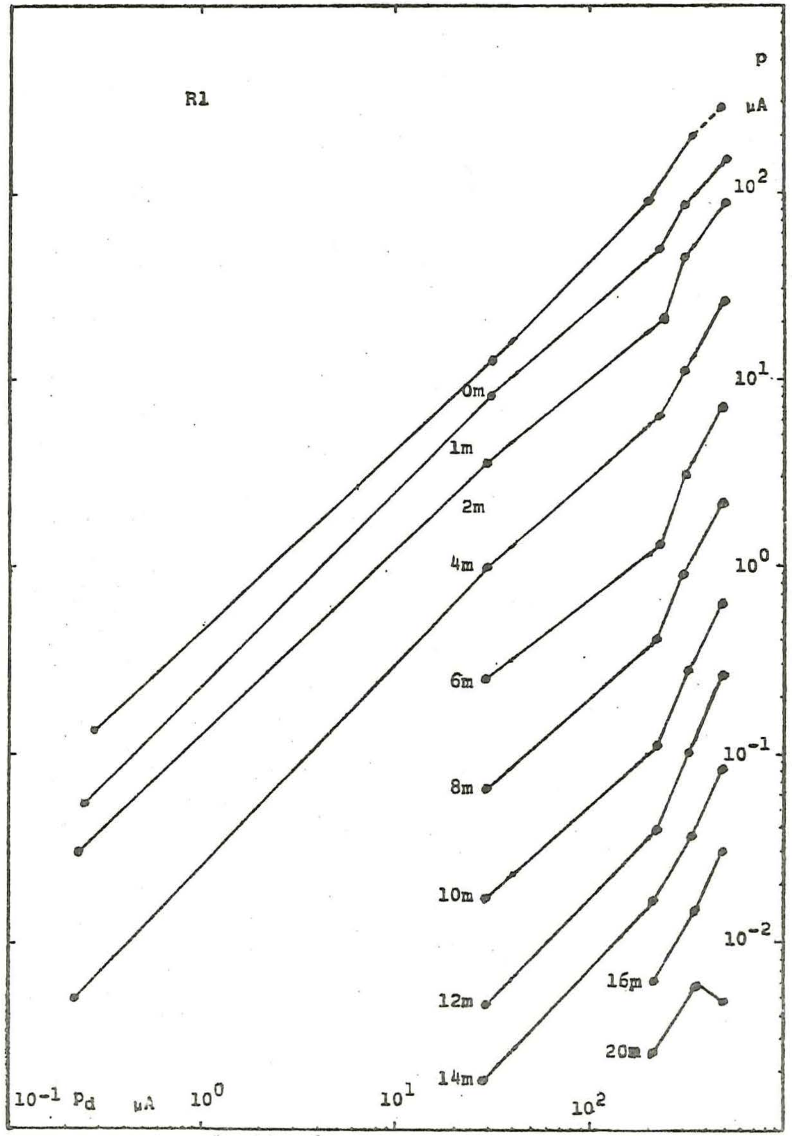

Fig. 7. p_{R1} as a function of p_d.
July 19, 1973.

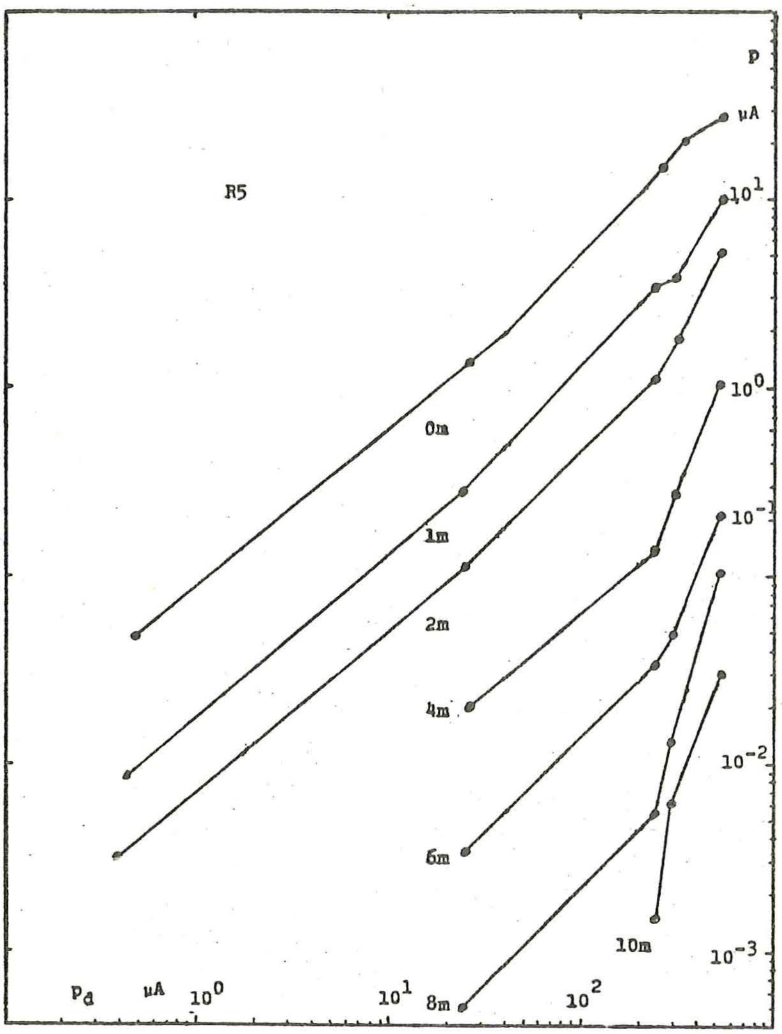

Fig. 8.
p_{R5} as a function of p_d. July 19, 1973.

Fig. 9.
p_{B12} as a function of p_d.
September 12, 1974.

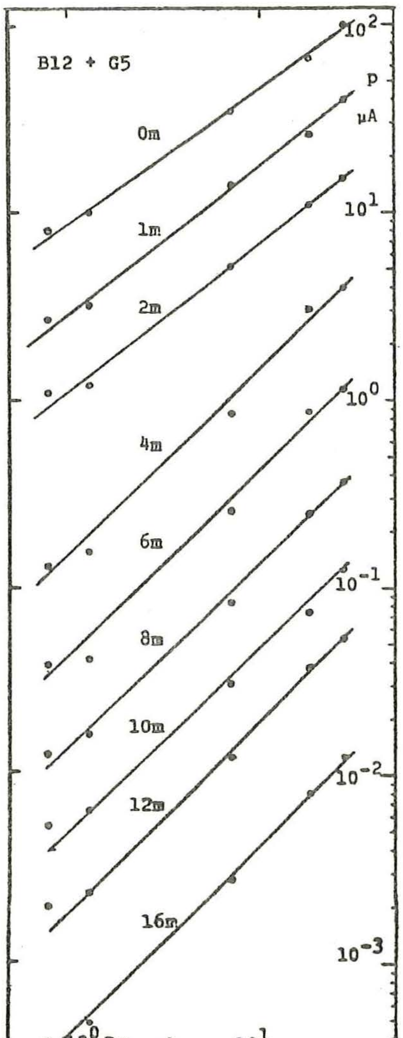

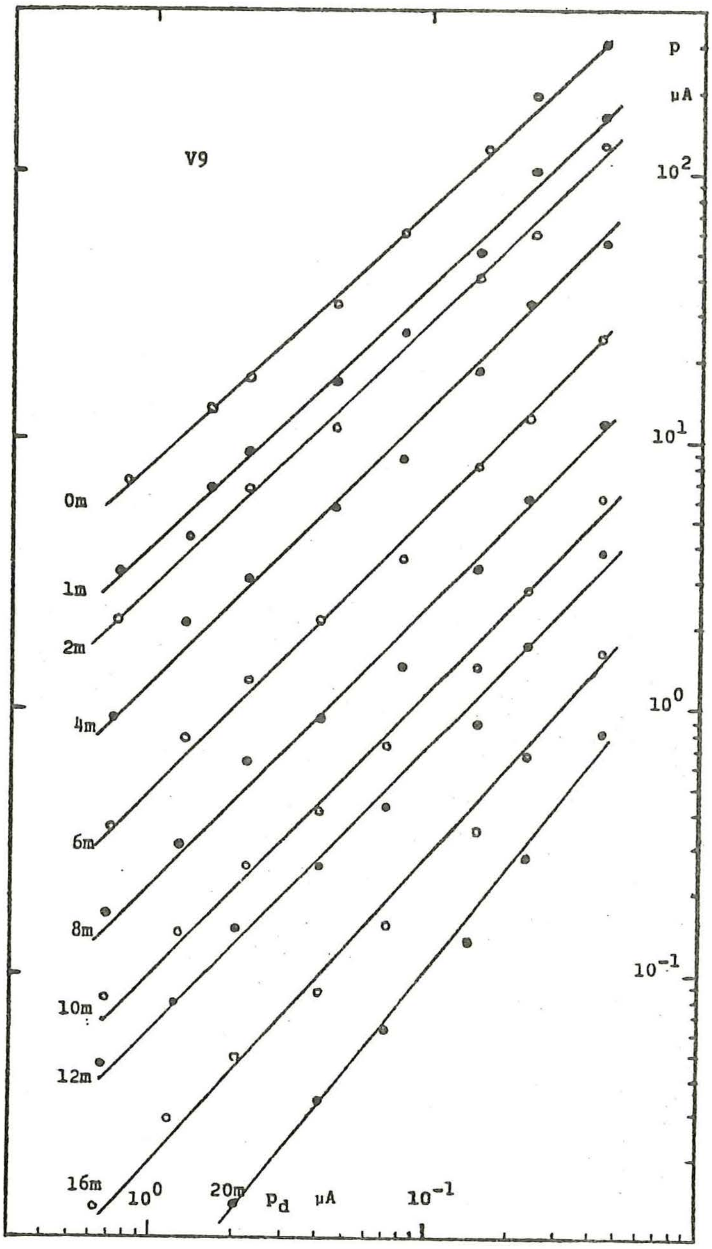

Fig. 10.
p_{V9} as a function of p_d. September 12, 1974.

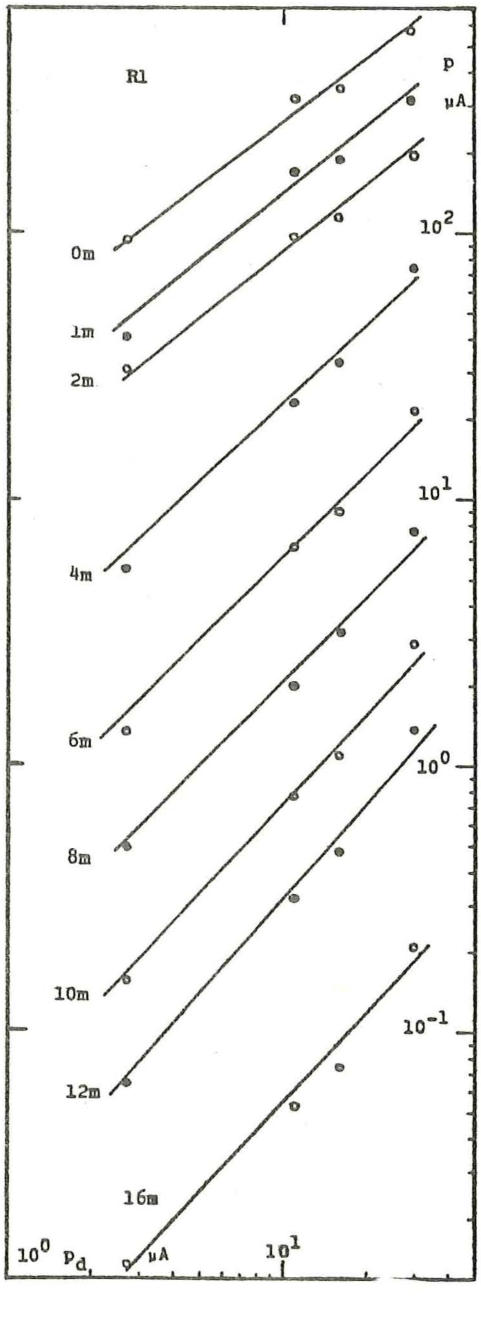

Fig. 11.
p_{R1} as a function of p_d. June 17, 1974.

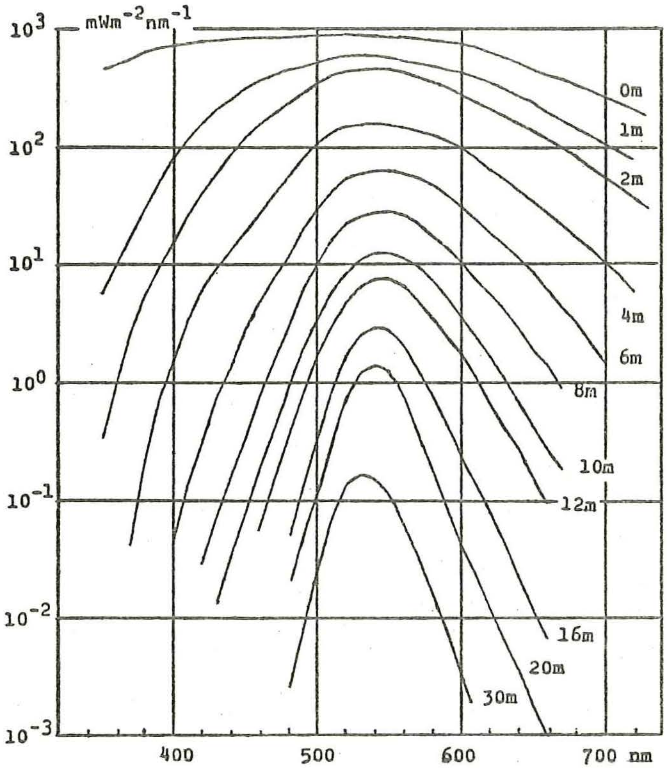

Fig. 12.
E_λ at 1400 hrs, h = 48°.

Fig. 13.
E_λ at 1600 hrs, h = 36°

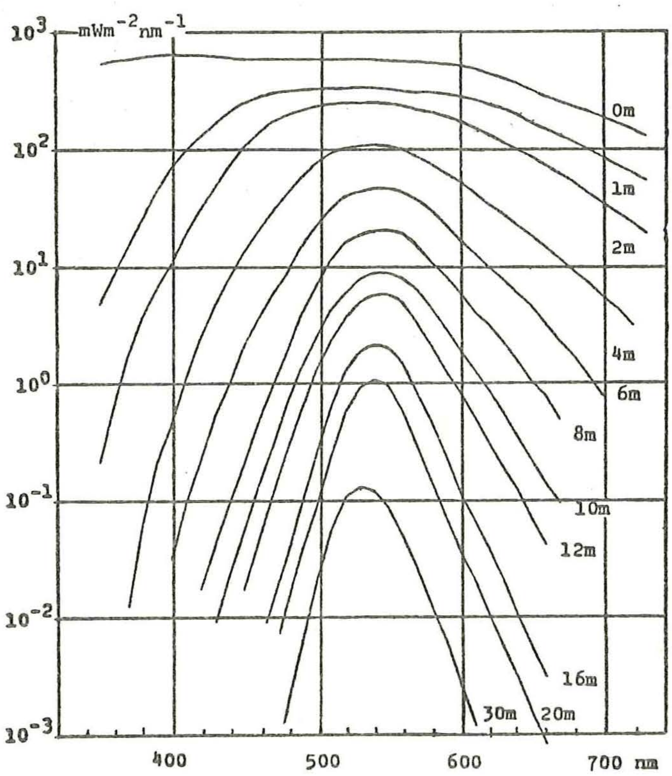

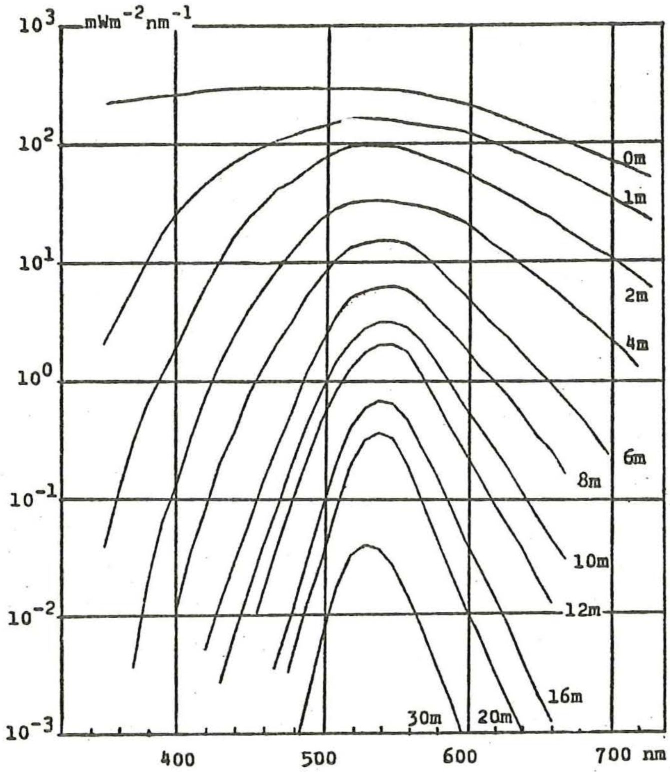

Fig. 14.
E_λ at 1800 hrs, h = 21°.

Fig. 15.
E_λ at 2000 hrs, h = 7°.

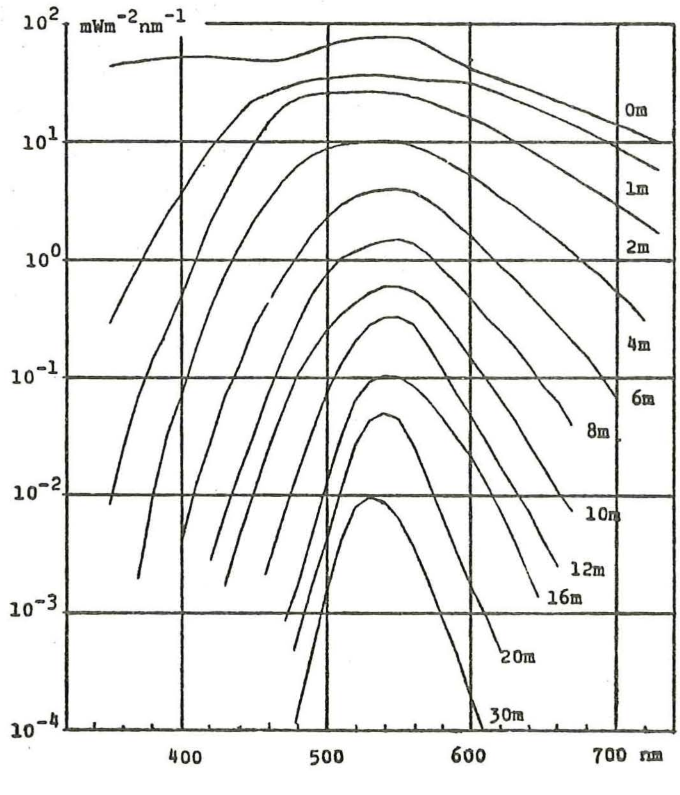

Fig. 16.
E_λ at 2200 hrs, h = -2^o.

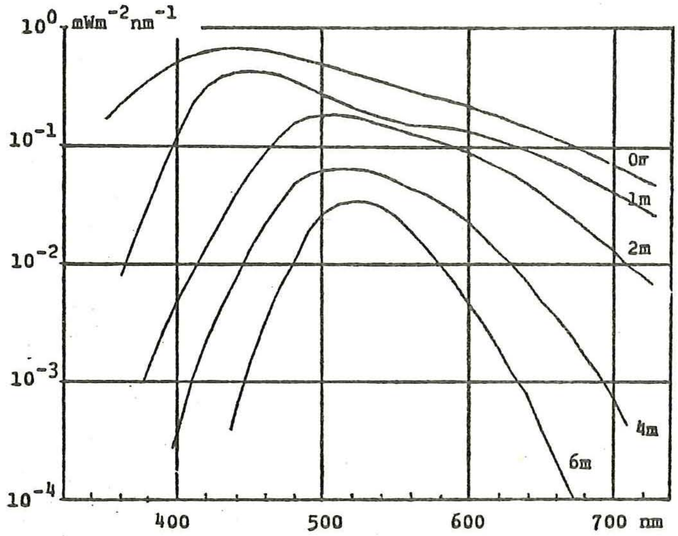

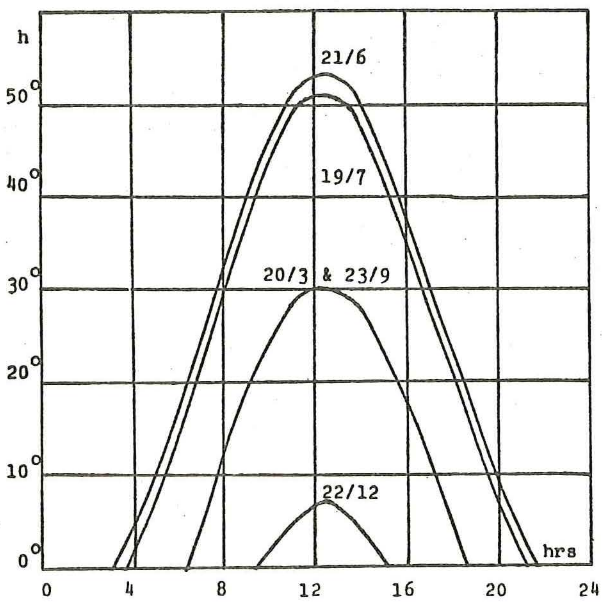

Fig. 17.
Solar elevation, h, as a function of local time at different dates.

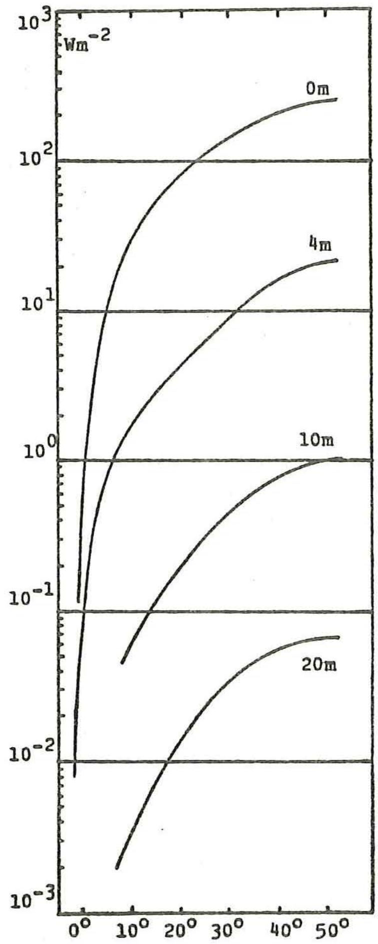

Fig. 18.
E as a function of solar elevation on July 19, 1973.

Fig. 19.
E as a function of local time.
July 19, 1973.

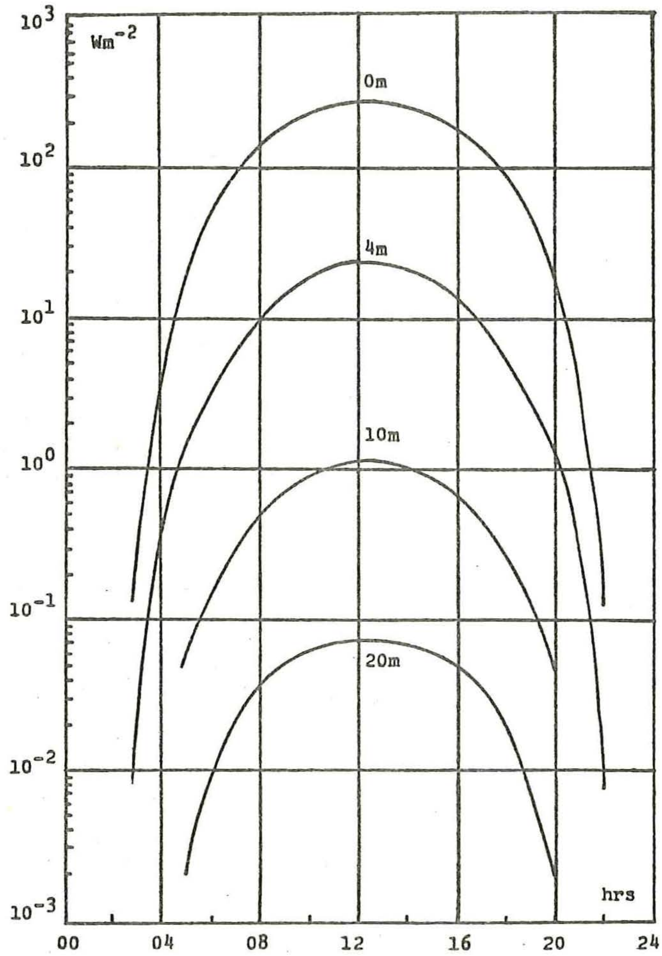

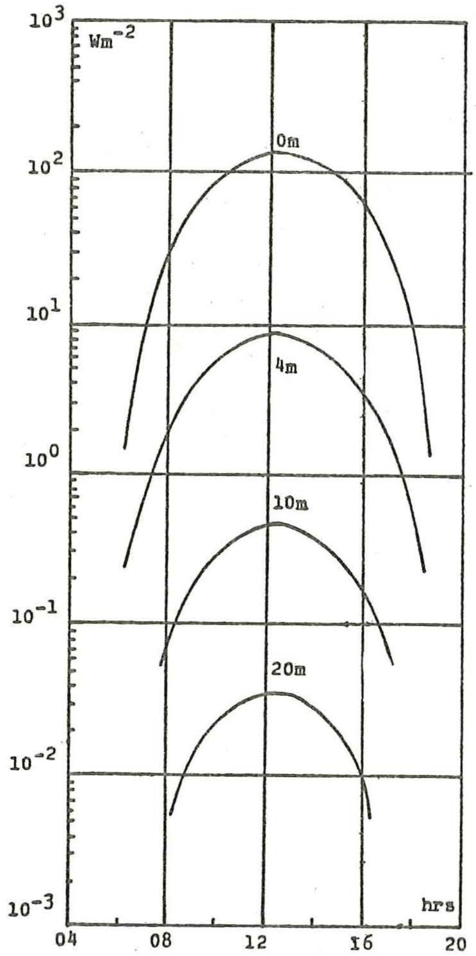

Fig. 20.
E as a function of local time
at vernal and autumnal equinox.

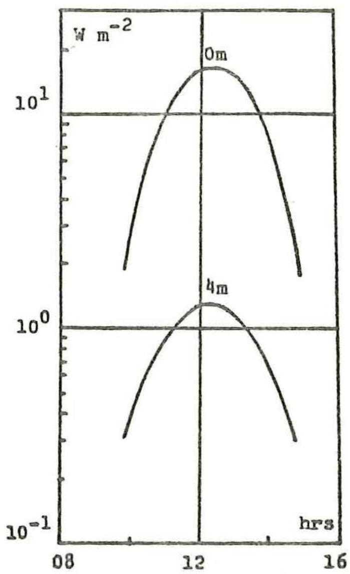

Fig. 21.
E as a function of local time at
winter solstice.

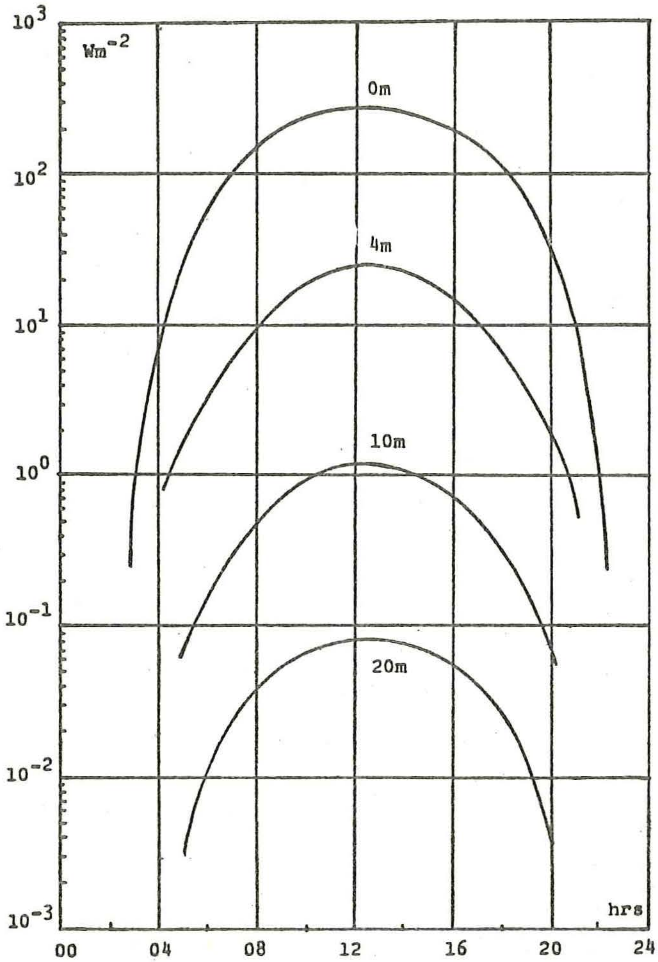

Fig. 22.
E as a function of local time at summer solstice.

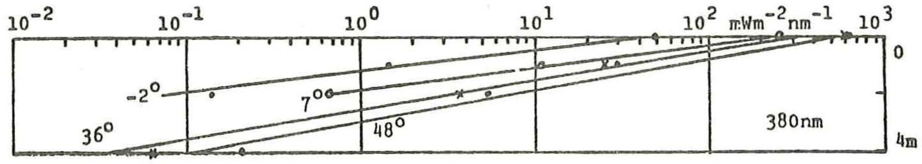

Fig. 23.
E_λ(380 nm) as a function of depth at different solar elevations.

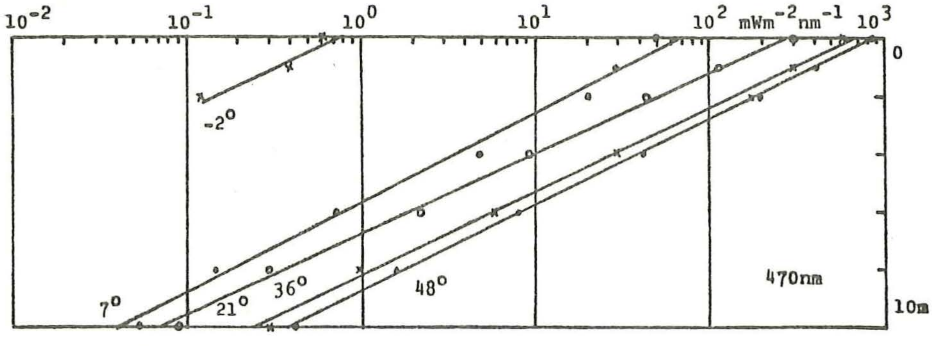

Fig. 24.
E_λ(470 nm) as a function of depth at different solar elevations.

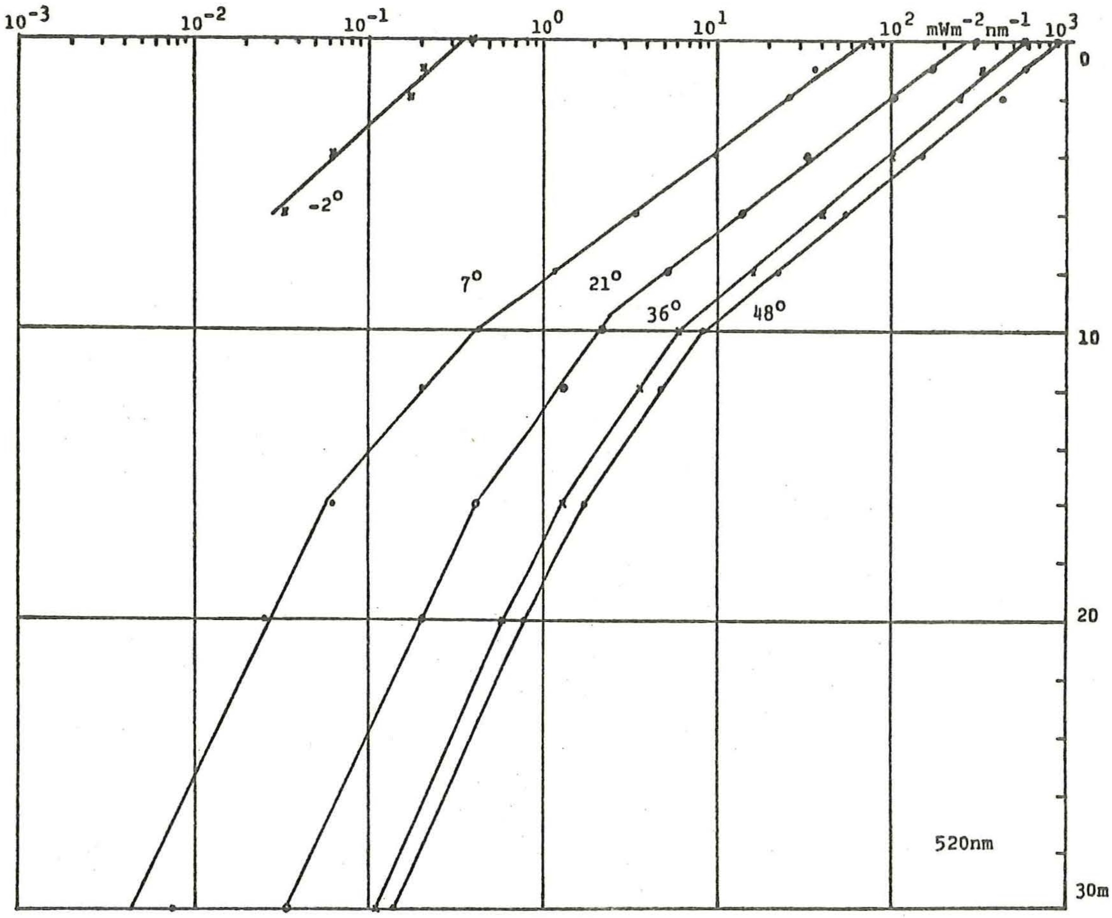

Fig. 25.
E_λ(520 nm) as a function of depth at different solar elevations.

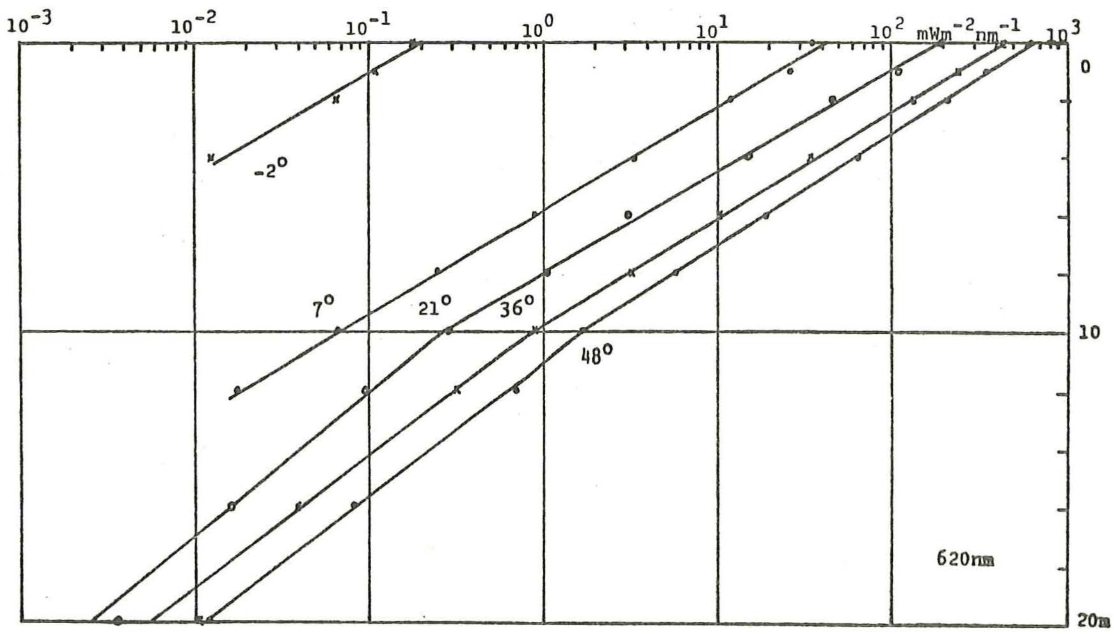

Fig. 26.
E_λ(620 nm) as a function of depth at different solar elevations.

Fig. 27.
K at different solar elevations. The hatched line denotes $\overline{K}$.

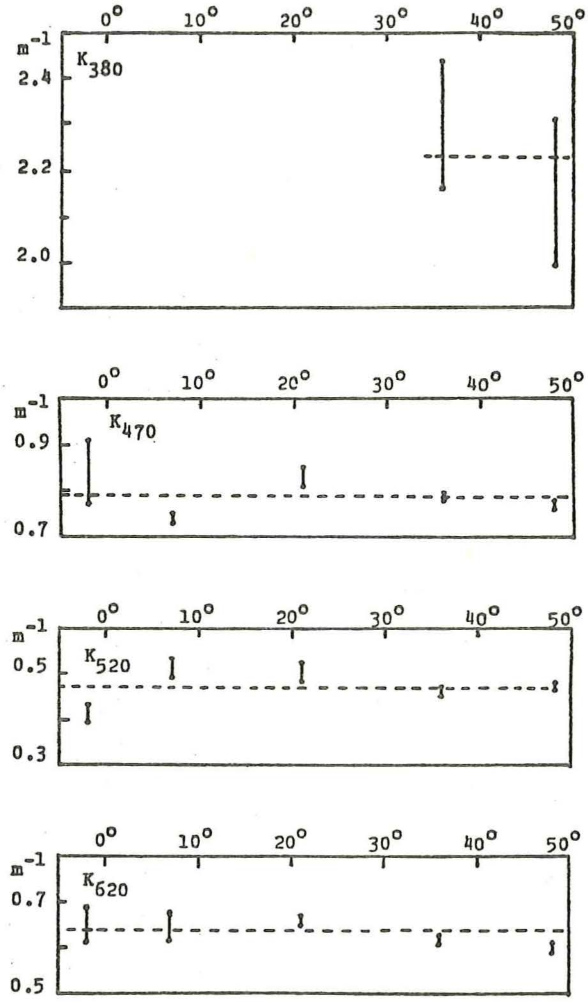

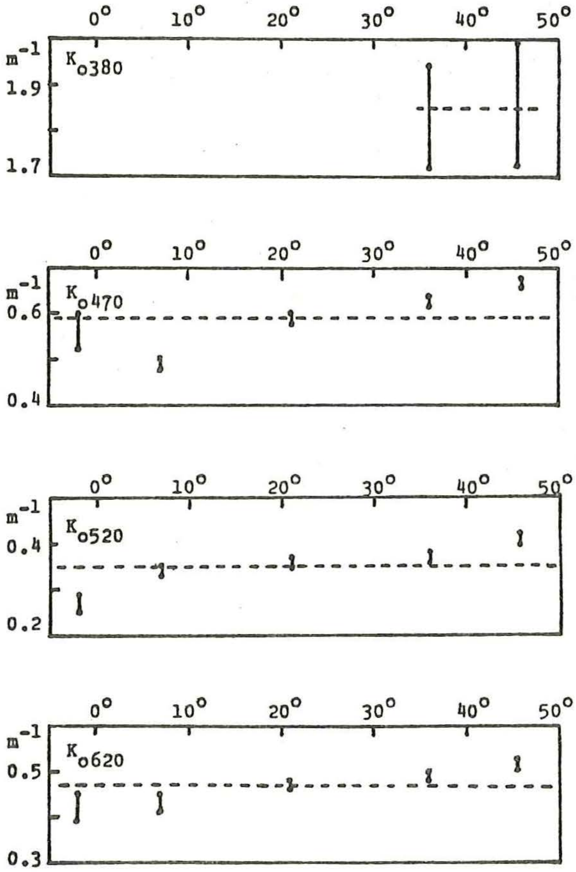

Fig. 28.
K_o at different solar elevations. The hatched line denotes $\overline{K}_o$.